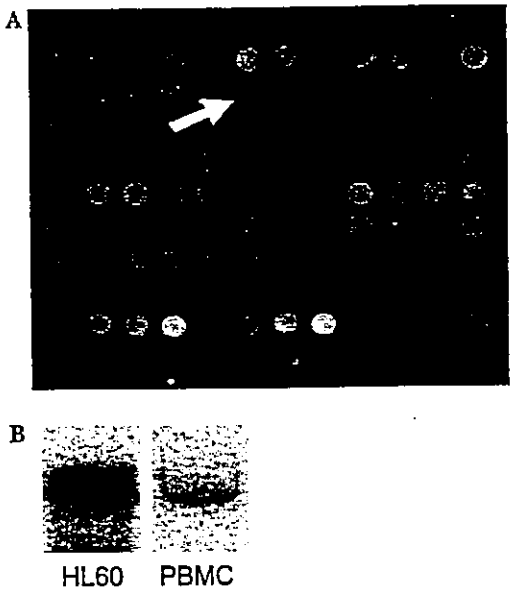

Fig. 1. Evaluation of the reliability of the cDNA microarray-based CGH method by comparison with Southern blotting. (A) Portion of typical array patterns of in-house microarrays (red, HL60; green, PBMC). The spot located by the white arrow indicates the c-myc gene. (B) Southern blot analysis of HL60 and PBMC DNA hybridized with c-myc probes. (C) DNA copy number of c-myc in HL60 cells, N-myc in IMR-32 cells, and the luciferase gene in RCF-26 cells determined by cDNA microarray and by Southern blotting. *Abbreviation:* F-Luc, firefly luciferase. (For interpretation of the references to color in this figure legend, the reader is referred to the web version of this paper.)

our method, we found that each of these genes was significantly amplified in their respective cell lines and that the estimated copy number determined by our cDNA array-CGH was well correlated with that from Southern blotting analysis (Fig. 1). Our cDNA array-CGH method also found that the DNA copy number of the p53 gene in HL60 cells was about half that in PBMCs (data not shown), in agreement with previously reported results [33].

Amplified and/or deleted genes detected by cDNA array-CGH

A typical scatter plot of intensities generated by Cy5 or Cy3 immobilized at the target sequence on the microarray slides is shown in Fig. 2. Using a fold-change of 1.8 or higher as the filtering criteria, we selected those genes with a >95% probability of being changed differentially. The seven hepatoma cell lines tested differed with respect to the number and identity of genes amplified or deleted (Table 1). As expected, we found that the HBV copy number was increased in the Hep3B and PLC/PRF/5 cell lines [1,34]. Although few genes were commonly amplified or deleted among the seven hepatoma cell lines, there were common biological characteristics among amplified or deleted genes in the individual cell lines. In the Hep3B and HepG2 cell lines, apoptosis-related gene copy numbers [e.g., glutathione-*S*-transferase T1 (GST T1), fas-associated via death domain (FADD), defender against apoptotic cell death (DAD1), and mammalian inhibitors of apoptosis homolog B (MIHB)] changed, whereas in the HLE cell line, cell adhesion and receptor molecule encoding gene copy numbers (e.g., integrin, glutamate receptor, and endothelin receptor) changed, and, in the PLC/PRF/5 cell line, the cytokine-related gene copy numbers (e.g., small inducible cytokine A2, interferon-α, and interferon regulatory factor 2) changed. Differences observed in amplified and deleted genes in these cell lines may reflect differences in their oncogenetic pathways and tumor phenotypes.

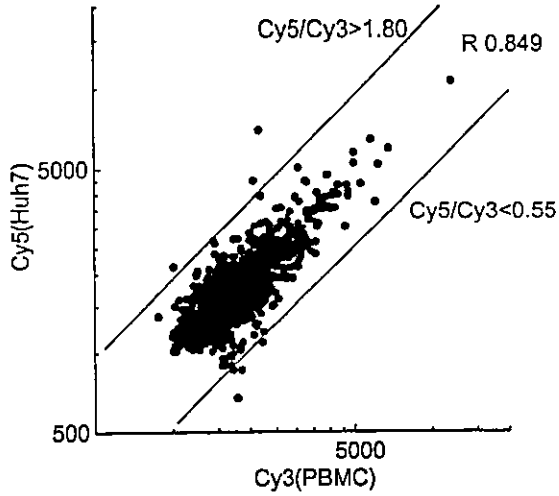

Fig. 2. Log_{10} (intensity of Cy5) and log_{10} (intensity of Cy3) of Huh7 cells are graphed on a scatter plot, and their linear relationship was examined statistically.

Southern blotting data

The changes in DNA copy number determined by our cDNA array-CGH were reevaluated by Southern blotting analysis (Fig. 3). In agreement with array-CGH results, we observed amplification of the HBV genome in the Hep3B and PLC/PRF/5 cell lines, and amplification of cyclin-dependent kinase 3 in Huh7 cells

Table 1
Genes amplified or deleted in seven hepatoma cell lines

Cell line	Gene name	Cy5/Cy3 (array-CGH)	Cy5/Cy3 (expression profiles)	Function	GenBank	Chromosome location
Huh7						
>1.80	RNA-binding motif protein 4 (RBM4)	3.15 ± 0.70	1.60	RNA-binding	NM_002896	11q13
	Cyclin-dependent kinase 3	2.19 ± 0.23	7.75	Cell cycle	NM_001258	17q22-qter
	Alpha platelet-derived growth factor receptor precursor	1.83 ± 0.40	1.77	Cell receptor	NM_006206	4q11-q13
<0.55	Inhibin, alpha	0.49 ± 0.05	1.28	Growth factor	NM_002191	2q33-q36
	Granzyme A	0.54 ± 0.11	0.49	Immune response	NM_006144	5q11-q12
Hep3B						
>1.80	Glutathione-*S*-transferase T1	8.91 ± 8.74	3.32	Apoptosis	NM_000853	22q11.23
	HBV-P	6.84 ± 7.16		Virus genome		
	HBV-full	3.60 ± 1.61		Virus genome		
	Homo sapiens CGI-137 protein	2.40 ± 1.66	1.46	Transcription factor	NM_003187	5q11.2-q13.1
	Fas-associated via death domain (FADD)	2.23 ± 0.39	1.54	Apoptosis	NM_003824	11q13.3
	H. sapiens PAC clone DJ0855D21	2.02 ± 0.90	1.48	PAC clone	AC004908	Unknown
	BCL-2 homologous antagonist/killer (BAK) protein	2.02 ± 1.37	1.81	Apoptosis	NM_001188	6p21.3
	Immunoglobulin mu-binding protein 2	1.91 ± 0.37	2.2	DNA-binding	NM_002180	11q13.2-q13.4
	Discs, large (*Drosophila*) homolog 1	1.88 ± 1.32	2.03	Guanylate kinase	NM_004087	3q29
	RNA-binding motif protein 4 (RBM4)	1.83 ± 0.04	4.02	RNA-binding	NM_006144	11q13
<0.55	Burkitt lymphoma receptor 1, GTP-binding protein	0.53 ± 0.18	2.27	Cell receptor	NM_032966	11q23.3
HepG2						
>1.80	Glutathione-*S*-transferase T1	2.70 ± 0.57	2.16	Apoptosis	NM_000853	22q11.23
	Defender against cell death (DAD1)	2.31 ± 0.27	1.46	Apoptosis inhibitor	NM_001344	14q11-q12
	Oxidase (cytochrome *c*) assembly 1-like	2.26 ± 0.19	2.66	Electron transport	NM_005015	14q11.2
	Transcriptional regulator ISGF3 gamma subunit	1.99 ± 0.53	11.1	Transcription factor	NM_006084	14q11.2
	Mammalian inhibitor-of-apoptosis homolog B (MIHB)	1.92 ± 0.85	0.59	Apoptosis inhibitor	NM_001166	11q22
	Guanine nucleotide-binding protein (G protein), alpha stimulating activity polypeptide 1	1.85 ± 0.31	1.85	Transcription factor	NM_080425	20q13.2-q13.3
<0.55	Nothing					
SKHep1						
>1.80	*H. sapiens* PAC clone DJ0855D21	2.10 ± 0.27	0.4	PAC clone	AC004908	Unknown
	Decorin	1.83 ± 0.17	1.28	Cell–cell interaction	NM_133503	12q13.2
<0.55	Inhibin, alpha	0.44 ± 0.02	0.34	Growth factor	NM_002191	2q33-q36
	H. sapiens insulin-like growth factor II receptor (IGF2R)	0.53 ± 0.01	0.3	Cell receptor	NM_000876	6q26
HLE						
>1.80	Interleukin enhancer-binding factor 1	2.90 ± 0.21	NA	Cytokine	NM_004514	17q25
	Integrin, beta 4	2.70 ± 0.45	NA	Cell–cell interaction	NM_000213	17q11-qter
	RB130 retinoblastoma-like 2	2.33 ± 0.47	NA	Protein kinase	NM_004203	16p13.11
	Glutamate receptor, ionotropic, AMPA 1	1.93 ± 0.26	0.8	Cell receptor	NM_000827	5q31.1
	E2D2	1.85 ± 0.38	1.95	Protein ligase	NM_003339	5q31.3
<0.55	Human vitamin K-dependent protein Z	0.38 ± 0.11	0.52	Protein-binding	NM_003891	13q34
	Endothelin receptor type B	0.40 ± 0.05	NA	Cell receptor	NM_000115	13q22
PLC/PRF/5						
>1.80	HBV-P	19.3 ± 4.62	NA	Virus genome		
	HBV-full	9.04 ± 5.36	NA	Virus genome		
	H. sapiens PAC clone DJ0855D21	2.81 ± 0.32	1.19	PAC clone	AC004908	Unknown
	Small inducible cytokine A2 (monocyte chemotactic protein 1, homologous to mouse Sig-je)	1.81 ± 0.02	4.05	Cytokine	NM_002982	17q11.2-q21.1
<0.55	Interferon-alpha	0.40 ± 0.10	1.44	Cytokine	NM_000605	9p22
	Interferon regulatory factor 2	0.45 ± 0.05	1.22	Cytokine	NM_002199	4q34.1-q35.1
	H. sapiens transcriptional coactivator p52	0.55 ± 0.29	1.13	Transcription factor	NM_033222	9p22.2
Huh6						
>1.80	Nothing					
<0.55	Nothing					

Notes. Clones showing a copy number ratio >1.80 were considered to be amplified and those with a copy number ratio <0.55 were considered to be deleted. The array-CGH data are expressed as means ± SD. *Abbreviation:* NA, data not available.

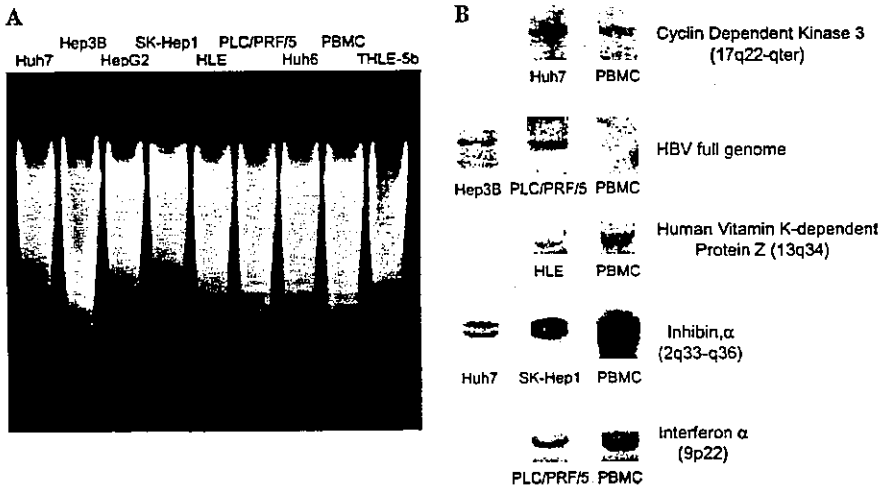

Fig. 3. Southern blot analyses of DNA from seven hepatoma cell lines. (A) Gel electrophoresis image of seven hepatoma cell lines and two normal cell lines. (B) Two amplified genes and three deleted genes in hepatoma cell lines, as shown by the cDNA array-CGH method.

by Southern blotting. Similarly, Southern blotting confirmed the deletion of inhibin α in Huh7 and SK-Hep1 cells, of human vitamin K-dependent protein Z in HLE cells, and of interferon-α in PLC/PRF/5 cells.

Comparison with expression microarray data

We proceeded to determine the relationship between genomic alterations and changes in mRNA expression in these cell lines (Table 1). We found that 40% of amplified genes were associated with mRNA overexpression and, conversely, 2–3% of overexpressed genes were accompanied by genomic alterations. When we plotted the global effect of copy number on gene expression, we found a direct relationship between these parameters (Fig. 4). Thus, changes in DNA copy number closely correlated with gene expression in these hepatoma cell lines.

Chromosome mapping

The chromosome locations of amplified and deleted genes were determined (Table 1, Fig. 5). In Hep3B cells, we observed a cluster of amplified and deleted genes at chromosome 11q13; whereas, in HepG2 cells, there was a cluster at 14q11. Similarly, we observed clusters at 5q31 in HLE cells and at 9p22 in PLC/PRF/5 cells. These results indicate that relatively long-range genomic DNA rearrangements take place within these cell lines. In addition to these clusters, DNA copy number

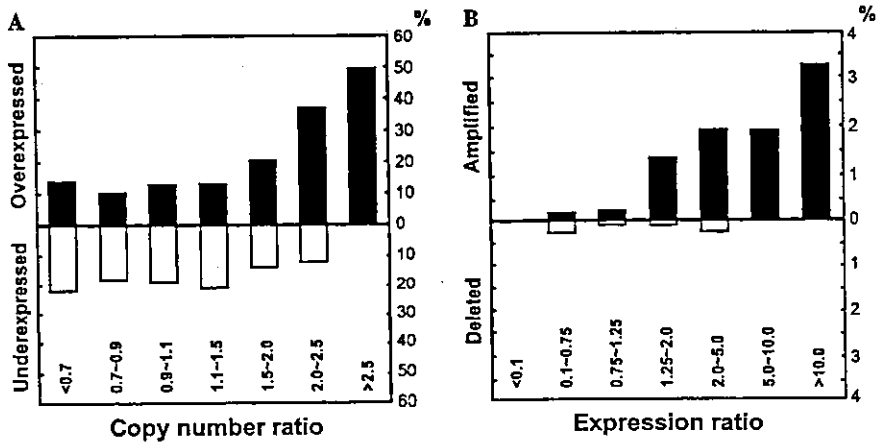

Fig. 4. Impact of gene copy number on global gene expression levels. (A) Percentage of over- and underexpressed genes (vertical axis) according to copy number ratios (horizontal axis). Threshold values used for over- and underexpression were >1.80 and <0.55, respectively. (B) Percentage of amplified and deleted genes according to expression ratios, using the same threshold values for amplification and deletion.

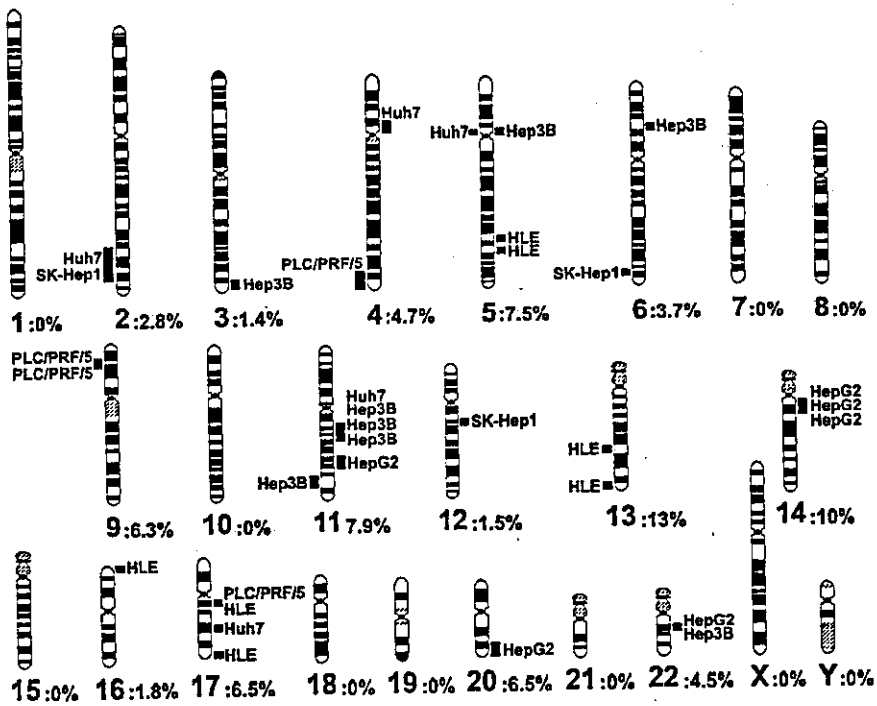

Fig. 5. Chromosome locations of genes amplified or deleted, as shown by cDNA array-CGH. Squares on the right side of each chromosome indicate genomic amplifications, squares on the left side indicate deletions. The percentages of genes amplified or deleted at each chromosomal location are indicated.

alterations were scattered at other chromosomal locations, reflecting genomic alteration in small regions, including multiple copies of single genes, in tumor cells. Overall, we found that there were many alterations in genes located on chromosomes 5 (7.5% amplified or deleted genes/analyzed genes), 11 (7.9%), 13 (13%), 14 (10%), and 17 (6.5%). In contrast, we did not identify any alterations on chromosomes 1 and 8 (Fig. 5), locations at which chromosomal alterations have been frequently observed in previous CGH analyses.

Genomic copy number profiling of hepatoma and non-hepatoma cells relative to clinical parameters

To determine the clinical relevance of our data, we evaluated the genomic copy number in each of these hepatoma and non-hepatoma cell lines with respect to their clinical parameters. Each hepatoma cell line in this study could be differentiated by various parameters, including HBV integration, AFP-production, and p53 mutation. Hierarchical clustering analysis of all copy number alterations did not differentiate these cell lines according to any clinical parameter, reflecting the high conservation of DNA copy number compared with mRNA expression. Using the class comparison method in BRB-Array tools ($p < 0.05$), however, we identified 57 genes that were differentially amplified between AFP-producing (40 genes) and AFP-negative (17 genes) cell lines (Fig. 6A, Table 2). Importantly, expression of mRNA encoded by these genes differentiated AFP-producing from AFP-negative cell lines, except for one (Huh7 cells, Fig. 6B), suggesting a physiological role of genomic copy number alterations in gene expression and the phenotype of these cell lines. Clinical parameters other than AFP-production, however, did not differentiate these cell lines.

Surprisingly, the genes differentially amplified in AFP-producing and AFP-negative cells were clustered at specific chromosomal locations (Table 2). Genes amplified in AFP-producing cell lines included interleukin-1 receptor types 1 (IL-1R1), 2 (IL-1R2), and transforming growth factor β receptor-1 (TGFβR1), located at cytokine receptor cluster 2q11-12; the apoptosis regulatory genes granzyme H, Bcl-w, and DAD1, located at 14q11-12; and the immune response genes cytokine receptor (EBI3), intercellular adhesion molecule 3 (ICAM3), CD79A, and interferon regulatory factor 3, located at 19q13. In AFP-negative cell lines, amplified genes were clustered at chromosomes 5q11-13 and 17q11. When these differentially expressed genes were classified by function, we found that many cell–cell interaction genes, including cytokine and chemokine receptors (IL-1R1, IL-1R2, TGFβR1, chemokine (C–C motif) receptor 5, IGF2R, EB13, and erythropoietin receptor), and cell adhesion molecules (collagen IX, ICAM3, Jagged1, and integrin), as well as cell cycle

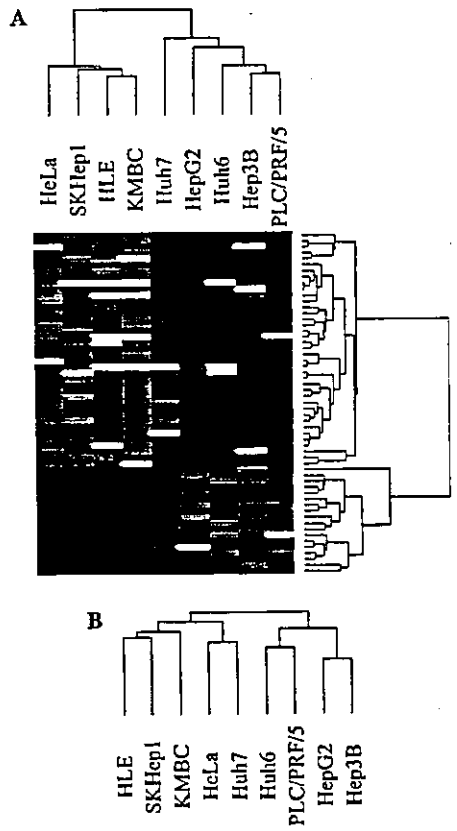

Fig. 6. Genes used to differentiate α-fetoprotein (AFP)-positive from AFP-negative cell lines. Using BRB-Array Tools Ver. 3.1.0 (http://linus.nci.nih.gov/BRB-ArrayTools.html), a modified *t* test was used to identify genes that could differentiate the AFP-positive hepatoma cell lines, Huh7, Hep3B, HepG2, PLC/PRF/5, and Huh6, from the AFP-negative hepatoma (SKHep1 and HLE) and non-hepatoma (HeLa and KMBC) cell lines. (A) Dendrogram of 57 genes determined by the class comparison method, showing the relatedness of genome gain or loss among these cell lines. (B) Expression of mRNA encoded by these 57 genes differentiated AFP-producing and AFP-negative cell lines, except for Huh7 cells.

(p19, KAP1, and B-myb) and apoptosis-related genes (granzyme H, Bcl-w, and DAD1), were up-regulated in AFP-producing cells.

Discussion

Microarray-based CGH was developed to detect genome-wide alterations in tumor samples [14]. We utilized cDNA as probes instead of BAC or PAC clones, making it easier to determine genes amplified and/or deleted in these cell lines and enabling us to evaluate the effect of changes in DNA copy number on mRNA expression [19]. In addition, the cDNA array-CGH method enabled us to detect changes in small regions of DNA, especially intron-less genes, including interferon-α and BCL-2 homologous antagonist/killer protein. Using cDNA probes eliminated binding to intron sequences of the genome, thus decreasing the background signal. We verified the reliability of our cDNA array-CGH method using cell lines known to have high copy numbers of c-myc (HL60), N-myc (IMR-32), and luciferase (RCF-26) genes, all of which were significantly amplified by our cDNA array-CGH method and shown to correlate with Southern blot results. Our cDNA array consisted of suitable gene sets for analyzing the hepatoma cell lines. Using this series of in-house cDNA microarrays, gene expression profiling clearly distinguished between AFP-positive and AFP-negative cell lines [23], differential gene expression in chronic hepatitis B and C tissue lesions was demonstrated [21], gene expression profiling of hepatocellular carcinoma was performed [22], and genes for systemic vascular complications were found to be differentially expressed in the livers of type 2 diabetic patients [35]. Thus, the cDNA microarray used in this study was equipped with gene sets suitable and advantageous for the evaluation of human liver-derived materials. Furthermore, the sensitivity and specificity of our cDNA microarray had been properly evaluated. As we previously reported, the sensitivity of our array system is sufficient to detect 10^3 copies/ml (in the case of plasmid DNA) to 10^5 copies/ml (in the case of serum HBV virus) of the HBV genome, which corresponds to 4–400 ng/ml of human genomic DNA [36]. The high sensitivity of our array system enabled us to detect gene amplification or deletion properly, as confirmed by Southern blotting in this study. To reduce non-specific binding of intronic sequences to the cDNA probe on the slide, genomic DNA preparation was modified from previously described methods. Specifically, nuclei were isolated from cells, mitochondrial DNA was removed, and the nuclei were sonicated before *Dpn*II restriction enzyme digestion. These changes increased the specificity and sensitivity of our cDNA array-CGH system.

Although few genes were amplified or deleted in common among the seven hepatoma cell lines analyzed, we found that there were common biological characteristics among the genes amplified or deleted in the individual cell lines. As the sharp contrast in function of the genes amplified and deleted in each cell line may reflect their different oncogenetic pathways and tumor phenotypes, a greater number of genes must be analyzed in these cell lines before more confident conclusions can be made.

In hepatoma cells, CGH analysis showed that the most frequent DNA copy number gains had been localized to 1p34.3-35, 1p33-34.1, 1q21-23, 1q31-32, 6p11-12, 7p21, 7q11.2, 8q24.1-24.2, 11q11-13, 12q11-13, 12q23, 17q11.2-21, 17q23-24, and 20p11.1-q13.2, whereas recurrent losses had been mapped to 3p12-14, 3q25, 4p12-14, 4q13-34, 5q21, 6q25-26, 8p11.2-23, 9p12-24, 11q23-24, 13q12-33, 14q12-13, 15q25-26, 18q11.2-22.2, and 21q21-22 [37]. Our data did not show amplified or deleted genes on chromosomes 1q or 8q where amplification had been

Table 2
Identification of 57 genes differentially amplified in AFP-producing and AFP-negative cell lines

Genes	Chromosome location	Fold (genome: AFP-producing cells/ AFP-negative cells)	Fold (expression: AFP-producing cells/ AFP-negative cells)	Function	GenBank
AFP-producing cell lines dominant					
Protein tyrosine phosphatase, non-receptor type 7	1q32.1	1.314	1.087	Signal transduction	NM_080588
MAX dimerization protein	2p13-p12	1.871	1.025	Transcriptional repressors	NM_002357
Ribosomal protein	2q11.1-q11.2	1.349	1.393	Housekeeping Genes	NM_014763
Interleukin 1 receptor 1	2q12	1.626	0.949	Cytokine	NM_003856
Interleukin 1 receptor 2	2q12-q22	1.359	0.807	Cytokine	NM_004633
TGFbeta receptor 1	2q12.1	1.315	0.797	Cell receptor	NM_004257
ERCC3	2q21	1.427	1.240	DNA repair	NM_000122
Homeobox protein HOX-D3	2q31-q37	1.627	1.087	Transcriptional factors	NM_006898
Chemokine (C–C motif) receptor 5	3p21	1.313	1.025	Cell receptor	NM_000579
Special AT-rich sequence-binding protein 1	3p23	1.301	0.726	Transcriptional factors	NM_002971
Sno oncogene snoN protein ski-related	3q26	1.326	0.948	Oncogenes	NM_005414
Epidermal growth factor	4q25	1.373	0.958	Growth factors	NM_001963
Collagen, type IX, alpha 1	6q12-q14	1.44	1.040	Cell–Cell interaction	NM_078485
Cytosolic acetoacetyl-coenzyme A thiolase	6q25-q27	1.347	2.234	Stress and toxicology response	NM_005891
IGF2R	6q26	1.4	1.270	Cell receptor	NM_000876
Paraoxonase 3	7q21.3	1.265	1.608	Metabolism	NM_000940
Deoxynucleotidyltransferase, terminal	9q34.3	1.427	1.433	Cell receptor	NM_002957
Granzyme H	14q11.2	2.503	0.942	Immune response	NM_033423
Ref-1	14q11.2-q12	1.468	1.375	DNA repair	NM_080648
Bcl-w	14q11.2-q12	1.424	1.057	Apoptosis	NM_004050
DAD1	14q11-q12	1.638	0.858	Apoptosis inhibitor	NM_001344
Chromosome 16 BAC clone CIT987SK-A-233A8	16	1.309	1.027	BAC clone	Unknown
p19	19p13	1.425	0.734	Cell cycle	NM_079421
Human protein phosphatase (KAP1)	19p13.2	1.45	1.077	Cell cycle	NM_005192
EB virus-induced gene 3 (EBI3)	19p13.3	1.319	0.927	Cytokine	NM_005755
Nuclear factor I/X (CCAAT-binding transcription factor)	19p13.3	1.304	1.037	Transcriptional factors	NM_002501
Erythropoietin receptor	19p13.3-p13.2	1.475	1.005	Cell receptor	NM_000121
Intercellular adhesion molecule 3 (ICAM 3)	19p13.3-p13.2	1.441	1.528	Cell–Cell interaction	NM_002162
CD79A antigen	19q13.2	1.329	0.969	Immune response	NM_021601
Interferon regulatory factor 3	19q13.3-q13.4	1.366	1.079	Cytokine	NM_001571
Jagged 1	20p12.1-p11.23	1.384	2.144	Cell–Cell interaction	NM_000214
B-myb	20q13.1	1.473	0.708	Cell cycle	NM_002466
Glutamate receptor, ionotropic, kainate 1	21q22.11	1.326	0.794	Cell receptor	NM_000830
Integrin, beta 2	21q22.3	1.368	1.088	Cell–Cell interaction	NM_000211
Glutathione-S-transferase T1	22q11.23	2.187	1.160	Metabolism	NM_000853
Crystallin, beta B1	22q12.1	4.905	0.906	Structural components	NM_001887
Leukemia inhibitory factor	22q12.2	1.431	0.800	Growth factors	NM_002309
ESTs	22q13.1	1.306	1.168	EST	NM_002110
HBV-P	—	8.496	2.188	Virus genome	—
HBV-full	—	3.294	2.394	Virus genome	—
AFP-negative cell lines dominant					
CD58 antigen	1p13	0.737	1.086	Immune response	NM_001779
Glucose transporter-like protein-III (GLUT3)	1p22-p21	0.762	3.791	Transcriptional factors	NM_006931
Endothelin 2	1p34	0.762	0.747	Vasoconstrictor	NM_001956
Corticotropin releasing hormone-binding protein	5q11.2-q13.3	0.697	1.117	Hormone regulator	NM_001882

(continued on next page)

Table 2 (*continued*)

Genes	Chromosome location	Fold (genome: AFP-producing cells/ AFP-negative cells)	Fold (expression: AFP-producing cells/ AFP-negative cells)	Function	GenBank
Granzyme A	5q11-q12	0.684	0.960	Immune response	NM_006144
XRCC4	5q13-q14	0.718	0.911	DNA repair	NM_022406
Human protocadherin 42	5q32-q33	0.697	0.308	Cell–Cell interaction	NM_032420
Human KIAA0056	11q25	0.787	0.839	Unidentified human genes	Unknown
P120 antigen	12p13	0.703	1.097	Cell Cycle	NM_006170
Myelodysplasia/myeloid leukemia factor 2 (MLF2)	12p13	0.764	1.178	Leukemia factor	NM_005439
Alpha-2-macroglobulin	12p13.3-p12.3	0.649	3.886	Cell–Cell interaction	NM_000014
HIF-1	14q21-q24	0.735	1.103	p53 Pathway	Unknown
Monocyte chemotactic protein 2	17q11.2	0.721	1.031	Chemokine	NM_005623
Ecotropic viral integration site 2B	17q11.2	0.71	0.707	Oncogene	NM_006495
CDC18	17q21.3	0.751	0.751	Cell Cycle	NM_001254
Topoisomerase (DNA) II alpha	17q21-q22	0.74	1.048	Transcriptional factors	NM_001067
Transmembrane 4 superfamily member 2	Xq11	0.69	1.109	Cell–Cell interaction	NM_004615

frequently observed in other CGH analyses [37,38]. This may be due to the relatively low number of analyzed genes located on chromosome 8, although many genes located on chromosome 1 have been analyzed (data were not shown). The other possibility is that our criteria used for identifying genes may have been too strict and may have failed to find genes located in these chromosome lesions. By setting over 1.5-fold as significant, several chromosome 1q or 8q genes were listed, but, in addition, many chromosome 11q or 17q genes were listed as well. The last possibility might be that the use of intron-less cDNA probe sequences reduced the sensitivity of gene alteration detection, alterations which involved both intron and exon sequences. We failed to detect c-myc amplification in Huh7 cells by Southern blotting using cDNA probes that had successfully detected c-myc amplification in HL60. It is possible that only portions of genes, such as c-myc intronic sequences, are amplified in Huh7 cells.

When we compared DNA copy number and mRNA expression of individual genes, we found that about 40% of amplifications and/or deletions were associated with changes in mRNA expression level. Other reports have hypothesized that global genome-wide analysis of expression profiles may reflect chromosomal aberrations in hepatoma [7]. These findings indicate that alterations in DNA copy number have a marked effect on gene expression in hepatoma cell lines. Among the differentially expressed genes in AFP-producing cells, as determined by hierarchical clustering [23], we found that 16 out of 325 genes were frequently changed at the genome-wide level (data was not shown). Thus, the data described in this report support our previous data.

We previously reported that the five AFP-producing hepatoma cell lines could be differentiated from two AFP-negative cell lines by their global gene expression profiles using cDNA microarrays [23]. In this study, we found that these AFP-producing and AFP-negative hepatoma cell lines could not be clearly differentiated by hierarchical clustering using all the genes analyzed. We were able to identify many genes that could differentiate AFP-producing from AFP-negative hepatoma cell lines. We found that many cell–cell interaction genes, including cytokine and chemokine receptors, cell adhesion molecules, and cell cycle and apoptosis-related genes, were up-regulated in AFP-producing cells. Inflammation-related cytokine receptor family genes were up-regulated in AFP-producing cells, suggesting that these receptors may serve to mediate growth and inflammatory signaling, although functional studies must be performed to confirm this hypothesis. Thus, these data strongly suggest that alterations in DNA copy number are common to AFP-producing and AFP-negative cells, and that alterations in these genes, accompanied by altered mRNA expression, might determine the specific phenotype of each cell line. Differential expression of many of these genes did not exceed the 1.8-fold threshold, suggesting that differences lower than 1.8-fold may have physiological significance. Considering that non-synchronized cell populations contain cells at various points in the cell cycle, gene amplification or deletion may not be correlated with mRNA over- or underexpression, especially in those cells undergoing DNA synthesis or those in the mitotic phase of the cell cycle.

In this study, we have demonstrated that cDNA array-CGH analysis is a sensitive method for identifying altered genes in hepatoma cell lines. Although we found that alterations in DNA copy number can be correlated with gene expression, other types of alterations, including single nucleotide polymorphisms (SNPs) and epigenetic methylation, should also influence gene

expression levels. The biological significance of these chromosomal alterations on tumorigenesis in HCC requires further study, including the analysis of a greater number of genes and the use of more primary tumor samples.

Acknowledgments

We thank Dr. Hiroshi F. Kawai for discussions concerning the manuscript; Dr. Teruyuki Ueda, Akemi Nakano, Junko Hara, and Masami Ueda for excellent technical assistance; and Professor Seishi Murakami, Associate Professor Motoaki Ohtsubo, and Dr. Nobuyuki Itoh for providing cDNA clones.

References

[1] C.C. Harris, Hepatocellular carcinogenesis: recent advances and speculations, Cancer Cells 2 (1990) 146–148.
[2] R. Romeo, M. Colombo, The natural history of hepatocellular carcinoma, Toxicology 181–182 (2002) 39–42.
[3] K. Okuda, Hepatocellular carcinoma: recent progress, Hepatology 15 (1992) 948–963.
[4] C.J. Chen, D.S. Chen, Interaction of hepatitis B virus, chemical carcinogen, and genetic susceptibility: multistage hepatocarcinogenesis with multifactorial etiology, Hepatology 36 (2002) 1046–1049.
[5] N.C. Popescu, Comprehensive genetic analysis of cancer cells, J. Cell. Mol. Med. 4 (2000) 151–163.
[6] K. Hashimoto, N. Mori, T. Tamesa, T. Okada, S. Kawauchi, A. Oga, T. Furuya, A. Tangoku, M. Oka, K. Sasaki, Analysis of DNA copy number aberrations in hepatitis C virus-associated hepatocellular carcinomas by conventional CGH and array CGH, Mod. Pathol. 17 (2004) 617–622.
[7] J.S. Lee, S.S. Thorgeirsson, Hepatology (2002) 1134–1143.
[8] A. Kallioniemi, O.P. Kallioniemi, J. Piper, M. Tanner, T. Stokke, L. Chen, H.S. Smith, D. Pinkel, J.W. Gray, F.M. Waldman, Detection and mapping of amplified DNA sequences in breast cancer by comparative genomic hybridization, Proc. Natl. Acad. Sci. USA 91 (1994) 2156–2160.
[9] O.P. Kallioniemi, A. Kallioniemi, J. Piper, J. Isola, F.M. Waldman, J.W. Gray, D. Pinkel, Optimizing comparative genomic hybridization for analysis of DNA sequence copy number changes in solid tumors, Genes Chromosomes Cancer 10 (1994) 231–243.
[10] E. Schrock, G. Thiel, T. Lozanova, S. du Manoir, M.C. Meffert, A. Jauch, M.R. Speicher, P. Nurnberg, S. Vogel, W. Janisch, et al., Comparative genomic hybridization of human malignant gliomas reveals multiple amplification sites and nonrandom chromosomal gains and losses, Am. J. Pathol. 144 (1994) 1203–1218.
[11] M.R. Speicher, G. Prescher, S. du Manoir, A. Jauch, B. Horsthemke, N. Bornfeld, R. Becher, T. Cremer, Chromosomal gains and losses in uveal melanomas detected by comparative genomic hybridization, Cancer Res. 54 (1994) 3817–3823.
[12] R.F. Suijkerbuijk, D.E. Olde Weghuis, M. Van den Berg, F. Pedeutour, A. Forus, O. Myklebost, C. Glier, C. Turc-Carel, A. Geurts van Kessel, Comparative genomic hybridization as a tool to define two distinct chromosome 12-derived amplification units in well-differentiated liposarcomas, Genes Chromosomes Cancer 9 (1994) 292–295.
[13] J.G. Bauman, J. Wiegant, P. Borst, P. van Duijn, A new method for fluorescence microscopical localization of specific DNA sequences by in situ hybridization of fluorochromelabelled RNA, Exp. Cell Res. 128 (1980) 485–490.
[14] D. Pinkel, R. Segraves, D. Sudar, S. Clark, I. Poole, D. Kowbel, C. Collins, W.L. Kuo, C. Chen, Y. Zhai, S.H. Dairkee, B.M. Ljung, J.W. Gray, D.G. Albertson, High resolution analysis of DNA copy number variation using comparative genomic hybridization to microarrays, Nat. Genet. 20 (1998) 207–211.
[15] E. Pestova, K. Wilber, W. King, Microarray-based CGH in cancer, Methods Mol. Med. 97 (2004) 355–375.
[16] K.K. Mantripragada, P.G. Buckley, T.D. de Stahl, J.P. Dumanski, Genomic microarrays in the spotlight, Trends Genet. 20 (2004) 87–94.
[17] W.W. Cai, J.H. Mao, C.W. Chow, S. Damani, A. Balmain, A. Bradley, Genome-wide detection of chromosomal imbalances in tumors using BAC microarrays, Nat. Biotechnol. 20 (2002) 393–396.
[18] S. Takeo, H. Arai, N. Kusano, T. Harada, T. Furuya, S. Kawauchi, A. Oga, T. Hirano, T. Yoshida, K. Okita, K. Sasaki, Examination of oncogene amplification by genomic DNA microarray in hepatocellular carcinomas: comparison with comparative genomic hybridization analysis, Cancer Genet. Cytogenet. 130 (2001) 127–132.
[19] E. Hyman, P. Kauraniemi, S. Hautaniemi, M. Wolf, S. Mousses, E. Rozenblum, M. Ringner, G. Sauter, O. Monni, A. Elkahloun, O.P. Kallioniemi, A. Kallioniemi, Impact of DNA amplification on gene expression patterns in breast cancer, Cancer Res. 62 (2002) 6240–6245.
[20] J.R. Pollack, T. Sorlie, C.M. Perou, C.A. Rees, S.S. Jeffrey, P.E. Lonning, R. Tibshirani, D. Botstein, A.L. Borresen-Dale, P.O. Brown, Proc. Natl. Acad. Sci. USA (2002) 12963–12968.
[21] M. Honda, S. Kaneko, H. Kawai, Y. Shirota, K. Kobayashi, Differential gene expression between chronic hepatitis B and C hepatic lesion, Gastroenterology 120 (2001) 955–966.
[22] Y. Shirota, S. Kaneko, M. Honda, H.F. Kawai, K. Kobayashi, Identification of differentially expressed genes in hepatocellular carcinoma with cDNA microarrays, Hepatology 33 (2001) 832–840.
[23] H.F. Kawai, S. Kaneko, M. Honda, Y. Shirota, K. Kobayashi, α-Fetoprotein-producing hepatoma cell lines share common expression profiles of genes in various categories demonstrated by cDNA microarray analysis, Hepatology 33 (2001) 676–691.
[24] C.D. Little, M.M. Nau, D.N. Carney, A.F. Gazdar, J.D. Minna, Amplification and expression of the c-myc oncogene in human lung cancer cell lines, Nature 306 (1983) 194–196.
[25] Y. Shiloh, J. Shipley, G.M. Brodeur, G. Bruns, B. Korf, T. Donlon, R.R. Schreck, R. Seeger, K. Sakai, S.A. Latt, Differential amplification, assembly, and relocation of multiple DNA sequences in human neuroblastomas and neuroblastoma cell lines, Proc. Natl. Acad. Sci. USA 82 (1985) 3761–3765.
[26] M. Honda, S. Kaneko, E. Matsushita, K. Kobayashi, G.A. Abell, S.M. Lemon, Cell cycle regulation of hepatitis C virus internal ribosomal entry site-directed translation, Gastroenterology 118 (2000) 152–162.
[27] A.M. Pfeifer, K.E. Cole, D.T. Smoot, A. Weston, J.D. Groopman, P.G. Shields, J.M. Vignaud, M. Juillerat, M.M. Lipsky, B.F. Trump, et al., Simian virus 40 large tumor antigen-immortalized normal human liver epithelial cells express hepatocyte characteristics and metabolize chemical carcinogens, Proc. Natl. Acad. Sci. USA 90 (1993) 5123–5127.
[28] M. Schena, D. Shalon, R.W. Davis, P.O. Brown, Quantitative monitoring of gene expression patterns with a complementary DNA microarray, Science 270 (1995) 467–470.
[29] M. Schena, D. Shalon, R. Heller, A. Chai, P.O. Brown, R.W. Davis, Parallel human genome analysis: microarray-based expression monitoring of 1000 genes, Proc. Natl. Acad. Sci. USA 93 (1996) 10614–10619.

[30] J.R. Pollack, C.M. Perou, A.A. Alizadeh, M.B. Eisen, A. Pergamenschikov, C.F. Williams, S.S. Jeffrey, D. Botstein, P.O. Brown, Nat. Genet. (1999) 41–46.
[31] E.M. Southern, Detection of specific sequences among DNA fragments separated by gel electrophoresis, J. Mol. Biol. 98 (1975) 503–517.
[32] M.R. Evans, A.L. Bertera, D.W. Harris, The Southern blot. An update, Mol. Biotechnol. 1 (1994) 1–12.
[33] D. Wolf, V. Rotter, Major deletions in the gene encoding the p53 tumor antigen cause lack of p53 expression in HL-60 cells, Proc. Natl. Acad. Sci. USA 82 (1985) 790–794.
[34] G.M. MacNab, J.J. Alexander, G. Lecatsas, E.M. Bey, J.M. Urbanowicz, Hepatitis B surface antigen produced by a human hepatoma cell line, Br. J. Cancer 34 (1976) 509–515.
[35] T. Takamura, M. Sakurai, T. Ota, H. Ando, M. Honda, S. Kaneko, Genes for systemic vascular complications are differentially expressed in the livers of type 2 diabetic patients, Diabetologia 47 (2004) 638–647.
[36] K. Kawaguchi, S. Kaneko, M. Honda, H.F. Kawai, Y. Shirota, K. Kobayashi, Detection of hepatitis B virus DNA in sera from patients with chronic hepatitis B virus infection by DNA microarray method, J. Clin. Microbiol. 41 (2003) 1701–1704.
[37] D.B. Zimonjic, C.L. Keck, S.S. Thorgeirsson, N.C. Popescu, Novel recurrent genetic imbalances in human hepatocellular carcinoma cell lines identified by comparative genomic hybridization, Hepatology 29 (1999) 1208–1214.
[38] N. Wong, P. Lai, S.W. Lee, S. Fan, E. Pang, C.T. Liew, Z. Sheng, J.W. Lau, P.J. Johnson, Assessment of genetic changes in hepatocellular carcinoma by comparative genomic hybridization analysis: relationship to disease stage, tumor size, and cirrhosis, Am. J. Pathol. 154 (1999) 37–43.

GASTROENTEROLOGY 2005;128:449–462

40

La Protein Is a Potent Regulator of Replication of Hepatitis C Virus in Patients With Chronic Hepatitis C Through Internal Ribosomal Entry Site–Directed Translation

MASAO HONDA, TAKEO SHIMAZAKI, and SHUICHI KANEKO
Department of Gastroenterology, Kanazawa University Graduate School of Medicine, Kanazawa, Japan

Background & Aims: Translation of hepatitis C virus is an essential step of viral replication and is mediated by an internal ribosome entry site. We previously reported that the hepatitis C virus internal ribosome entry site is most active during the synthetic (S) or mitotic (M) phases and lowest during quiescent (G_0) phase. Here, we investigated host factors responsible for the regulation of the hepatitis C virus internal ribosome entry site. *Methods:* We synchronized the cell-cycle progression and evaluated gene-expression dynamics of host factors and kinetics of hepatitis C virus internal ribosome entry site activity in cells at various points during the cell cycle by using a complementary DNA microarray. We also validated the significance of identified host factors on hepatitis C virus replication in vivo. *Results:* Hepatitis C virus internal ribosome entry site activity correlated with a gene cluster induced in the S and G_2/M phases. It is interesting to note that most initiation factors known to bind or interact with the hepatitis C virus internal ribosome entry site [poly(rC)-binding protein 2, polypyrimidine tract binding protein, eukaryotic initiation factor 3, eukaryotic initiation factor 2γ, eukaryotic initiation factor 2β, La protein, and heterogenous nuclear ribonucleoprotein L] were induced during the S and G_2/M phases. Expression of La protein, polypyrimidine tract binding protein, and eukaryotic initiation factor 3 (p116, p170) were predominantly repressed in G_0 phase and induced in S and G_2/M phases. Suppression or overexpression of La protein and polypyrimidine tract binding protein in RCF-26 significantly changed hepatitis C virus internal ribosome entry site activity. In the livers of patients with chronic hepatitis C, expression of La protein was significantly increased and correlated with the amount of hepatitis C virus RNA. *Conclusions:* Hepatitis C virus uses host factors induced during cell division but not during quiescence for replication. Of these, La protein is a potent regulator and enhances hepatitis C virus replication in regenerating hepatocytes in patients with chronic hepatitis C.

Hepatitis C virus (HCV), a positive-strand enveloped RNA virus, belongs to the genus *Hepacivirus* of the family Flaviviridae.[1] The human liver infected with HCV develops chronic hepatitis, cirrhosis, and, in some instances, hepatocellular carcinoma.[1,2] Although a combination of ribavirin and interferon has become a popular means of treating infected patients, the results are often unsatisfactory, especially in patients with a high viral load.[3–6] Identification of host factors that regulate HCV replication in infected patients could be helpful in the development of a novel antiviral treatment strategy.

Translation of the polyproteins of the HCV RNA genome is an essential step in viral replication and is supposed to be a fruitful target of new antiviral treatment strategies, such as antisense oligonucleotide (oligo) or small interference RNA. Translation of HCV is initiated by a highly structured RNA segment, the internal ribosome entry site (IRES), that occupies most of the 5′-nontranslated (5′-NTR) RNA.[7–15] The translation machinery of HCV is simple and, because it is a prokaryote, requires only the ribosomal 40S subunit, the eukaryotic initiation factor (eIF)2/guanosine triphosphate/Met-transfer RNA complex, and eIF3 to initiate translation.[7] In contrast, cap-dependent translation is more complex and requires additional canonical initiation factors, such as eIF4E, eIF4G, eIF4A, and eIF4B.[7] Many other noncanonical translation initiation factors, such as La protein,[16,17] polypyrimidine tract binding protein (PTB),[18] heterogeneous nuclear ribonucleoprotein L (RNPL),[19] poly(rC)-binding protein (PCBP)-2,[20] and ribosomal protein S9,[7] interact with HCV IRES and might regulate HCV translation. Thus, the machineries of cap-dependent and HCV IRES–directed translation

Abbreviations used in this paper: CMV, cytomegalovirus; eIF, eukaryotic initiation factor; FBS, fetal bovine serum; FL, firefly luciferase; IRES, internal ribosome entry site; nt, nucleotide; 5′-NTR, 5′ nontranslated region; oligo, oligonucleotide; PABPC, poly(A)-binding protein, cytoplasmic; PCBP, poly(rC)-binding protein; PTB, polypyrimidine tract binding protein; RL, *Renilla* luciferase; RNPL, heterogeneous nuclear ribonucleoprotein L; RTD, real-time detection; RT-PCR, reverse-transcription polymerase chain reaction; SOM, self-organizing map.

0016-5085/05/$30.00
doi:10.1053/j.gastro.2004.11.064

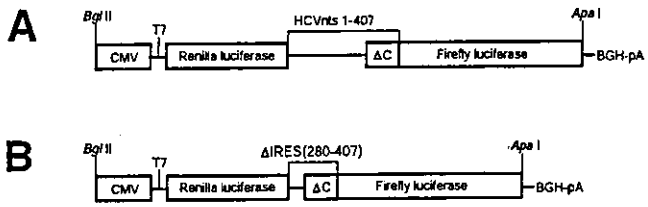

Figure 1. Organization of the transcriptional unit of plasmid pRL-HL and pRL-(ΔIRES)-HL. (*A*) Plasmid pRL-HL[22] contains a dicistronic CMV transcriptional cassette in which upstream *Renilla* and downstream firefly luciferase genes are separated by the complete 5′-NTR and 66-nt core sequence of HCV (nts 1–407; strain 1b) placed in the intercistronic space. (*B*) Plasmid pRL-(ΔIRES)-HL was the control plasmid of pRL-HL in which the functional HCV IRES element (nts 1–279) was deleted. CMV, cytomegalovirus promoter; T7, Bacteriophage T7 RNA polymerase promoter; BGH-pA, bovine growth hormone polyadenylation signal.

can be differentiated in terms of requirements for canonical and noncanonical initiation factors.[21]

We previously found that HCV IRES activity varies during the cell cycle and is greatest during the synthetic (S) or mitotic (M) phases and lowest during the quiescent (G_0) phase.[22] These findings suggest that HCV translation is regulated by cellular proteins that vary in abundance during the cell cycle and that viral replication is enhanced by factors that stimulate the regeneration of hepatocytes in patients with chronic hepatitis C. This finding implies that inflammation and the resulting increased turnover in hepatocytes may increase the number of actively dividing hepatocytes, resulting in increased IRES activity and enhanced HCV replication.

This study profiles the expression of cellular proteins during cell-cycle progression and identifies factors responsible for cell cycle–dependent HCV IRES–directed translation. We evaluated whether those factors are in fact related to HCV replication in the livers of patients with chronic hepatitis C.

Materials and Methods

Plasmids

Plasmid pRL-HL contains a dicistronic cytomegalovirus (CMV) transcriptional cassette in which an upstream *Renilla* luciferase (RL) gene and a downstream firefly luciferase (FL) gene are separated by the complete 5′-NTR and 66-nucleotide (nt) core sequence of HCV (nts 1–407 of a genotype 1b strain) placed within the intercistronic space[22] (Figure 1*A*). Plasmid pRL-(ΔIRES)-HL was the control plasmid of pRL-HL in which the functional HCV IRES element (nts 1–279) had been deleted (Figure 1*B*). This plasmid was constructed by subcloning the 1.82-kilobase *StuI*/*ApaI* fragment of pRL-HL (containing the deleted HCV IRES element [nts 280–341 of the HCV-1b 5′-NTR sequence and 66 nts of the core sequence] fused directly to FL) into the multiple cloning site of pBluescript IISK (Stratagene, La Jolla, CA). A 1.82-kilobase *NotI*/*ApaI* fragment was subsequently excised from this plasmid and cloned into the *NotI*/*ApaI* site of pRL-HL.

The La expression vector pCMV-La was constructed as previously described.[23] The PTB expression vector pRC/CMV-PTB, the RNPL expression vector pcDNA3-myc-hnRNPL, and the PCBP-1 and PCBP-2 expression vectors pcDNA3-myc-haCP1 and pcDNA3-myc-haCP2 were provided by Dr. Stanley M. Lemon,[24] Dr. Gideon Dreyfuss,[25] and Dr. Stephen A. Liebhaber,[26] respectively. Dr. John W. B. Hershey provided the eIF2γ full-length clone in pSP72.[27] We constructed the eIF2γ expression vector pCMV-eIF2-γ by excising the *Eco*RI and *Eco*RI fragment of full-length coding sequences and cloning into *Eco*RI of pCR 3.1 (Invitrogen, San Diego, CA) under the control of the CMV promoter. Dr. Keith Johnson provided the eIF3 p170 full-length clone in PUC19.[28] We constructed the eIF3 p170 expression vector pCMV-eIF3 p170 by excising the *Kpn*I and *Sna*BI fragment of full-length coding sequences and cloning into *Kpn*I and *Eco*RV of pCR 3.1 under the control of the CMV promoter. The complementary DNA (cDNA) of ribosomal protein S9 was cloned by reverse-transcription polymerase chain reaction (RT-PCR) of total RNA isolated from Huh-7 cells by using sense (5′-ACGGTGGAAGCGGACG-CAACATGCCAGTGG-3′) and antisense (5′-GGGACAG-GTGGACTTAATCCTCCTCCTCGTCG-3′) primers. The resultant cDNA was cloned into the TOPO TA cloning vector (Invitrogen), and nt sequences were confirmed. The expression vector pCMV-S9 was constructed by excising and cloning *Hin*dIII and *Xho*I fragments from TOPO TA into the same sites of pCR 3.1.

Cell Lines

The RCF-26 was a stably transformed cell line from Huh-7 cells (human hepatocellular carcinoma cells) that constitutively express dicistronic RNA transcripts containing sequences encoding 2 reporter proteins, RL and FL, separated by a functional HCV IRES[22] (Figure 1*A*). The ΔRCF-9 was a stably transformed cell line from Huh-7 cells that constitutively expressed dicistronic RNA transcripts in which the functional HCV IRES element (nts 1–279) had been deleted (Figure 1*B*).

Overexpression of Canonical and Noncanonical Initiation Factors in RCF-26

The RCF-26 cells were cultured in Dulbecco's modified Eagle medium (Gibco BRL, Gaithersburg, MD) containing 10% fetal bovine serum (FBS), 1% penicillin/streptomycin, and 400 μg/mL of Geneticin (active compound) (Gibco BRL, Gaithersburg, MD). Cells cultured in a 5% CO_2 incubator at 37°C were transfected with 0.5–1.0 μg of plasmid DNA by using FuGENE 6 (Roche Molecular Biochemicals, Basel, Switzerland) according to the manufacturer's instructions. After 24–48 hours of transfection, the cells were harvested, and reporter genes were assayed.

Reporter Gene Assays

Cells cultured in 10- or 15-cm dishes in Dulbecco's modified Eagle medium containing 10% FBS were trypsinzed. A quarter of the cells were lysed in 1 mL of passive lysis buffer (25 mmol/L Tris-phosphate [pH 7.8], 2 mmol/L dithiothreitol, 2 mmol/L 1,2-diaminocyclohexane-N,N,N′,N′-tetraacetic acid, 10% glycerol, and 1% Triton X-100). RL and FL activities were measured in 20 μL of cell lysate by using the Dual-Luciferase Reporter Assay System (Promega, Madison, WI). Total RNA was isolated from the remainder and processed for analysis by cDNA microarray, Northern blotting, and real-time detection (RTD) PCR.

Antisense Oligodeoxynucleotide

We designed respective antisense phosphorothioate oligos that were complementary to the sequence from 5 nts upstream to 15 downstream of the predicted translational initiation site of the La protein, PTB, eIF3 p170, eIF2γ, RNPL, poly(A)-binding protein, cytoplasmic 1 (PABPC-1), PCBP-2, and ribosomal protein S9 gene. The nt sequences of antisense oligos were 5′-GCCATTACGGCTATCTTTAA-3′ for La protein, 5′-TCCATGGCACACAGAGCAGA-3′ for PTB, 5′-GGCATTTTCCGGCCTCTGAA-3′ for eIF3 p170, 5′-CCAGCTTCTCCGCCCGCCAT-3′ for eIF2γ, 5′-ACCATCGCTCCCGACCGCCT-3′ for RNPL, 5′-TTCATCTCGGCACGGCTGCC-3′ for PABPC-1, 5′-TCCATGTCGAGCAGTGTTCT-3′ for PCBP-2, and 5′-GGCATGTTGCGTCCGCTTCCGCC-3′ for ribosomal protein S9. Positive and negative controls consisted of an antisense oligo for the 5′ region of HCV (nt 330–350), 5′-GTGCTCATGGTGCACGGTCT-3′,[29] and the randomized oligo, 6961, 5′-TACGTTTCTATGTCGATGGG-3′,[29] respectively. Oligodeoxynucleotides (0.5–1.0 μmol/L) were added to the medium by using the FuGENE6 transfection reagent (Boehringer Mannheim, Mannheim, Germany), and the cultures were incubated for 24 hours. Cells were harvested, and HCV IRES activity was evaluated by assaying the reporter genes. To validate repressed targeted gene expression, 1 μg of total RNA was amplified by RT-PCR with specific primers for La protein, PTB, eIF3 p170, and ribosomal protein S9. The internal control was the level of β-actin expression.

Synchronization of Cell Growth and Analysis of Cellular DNA Content

To examine the relationship between HCV IRES–directed translation and cell growth, RCF-26 cells and ΔRCF-9 cells were incubated in 15-cm dishes with low serum or at confluence for 24–48 hours. RCF-26 cells and ΔRCF-9 cells in 10-cm dishes were synchronized at the G_1/S phase border by starvation for 24 hours in medium containing 0.1% FBS, followed by a wash and an 18-hour incubation in medium containing 10% FBS and 2.5 μg/mL aphidicolin. Aphidicolin was removed from the synchronized cells by washing and adding fresh medium containing 1% FBS. The cells were harvested at 3-hour intervals over 48 hours to assess the cell-cycle phase and reporter enzyme activities. The cell-cycle phase distribution in each sample cell population was determined by measuring the DNA content of individual cells by flow cytometry.[22]

Complementary DNA Microarray Analysis

We profiled gene expression in cells at different phases of the cell cycle by cDNA microarray analysis. We reconstructed the gene set of cDNA microarray slides containing 1080 cDNA clones[30] by adding canonical and noncanonical initiation factors. The new microarray included La protein,[16] PTB,[18] eIF2β,[31] eIF2γ,[31] eIF3 p116, eIF3 p170,[32] RNPL,[19] ribosomal protein S9,[7] PCBP-2,[20] PABPC-1,[33] and cell division cycle 2–like 1 (PITSLRE proteins)[34] that bind HCV or other viral IRES structures and might affect the IRES activity. Other canonical initiation factors, such as eIF1A, eIF2A, eIF4A, eIF4B, eIF4E, and eIF5,[7,21,35] were also included to analyze cap-dependent translation machinery.

Total RNA (50 μg) isolated from serum-starved or confluent cells (10% FBS and at 60%–70% cell density) was labeled with a fluorescent dye for the cDNA microarray.[30,36,37] To profile gene expression in cells during the cell cycle, total RNA was periodically extracted from synchronized cells at 3, 9, 15, 18, 24, 30, 36, and 42 hours released from aphidicolin block (G_1/S border). After 1 round of amplification, antisense RNA was labeled and hybridized with the cDNA microarray.[30,36,37] Images were acquired, and cDNA microarray slides were analyzed as previously described.[30,36,37] A 1-dimensional self-organizing map (SOM) was constructed to cluster genes with a similar expression profile throughout cell-cycle progression (Cluster and Tree view; http://www.microarrays.org.html/software).

Northern Blotting

We evaluated La protein, PTB, and albumin expression in cultured cells and in tissue samples by Northern blotting. Total RNA (20 μg) was separated on denaturing agarose/formaldehyde gels, transferred to a membrane, and hybridized with specific probes under standard conditions.

Western Blotting

RCF-26 cells seeded in a 10-cm dish were grown to subconfluency and washed twice with phosphate-buffered saline. Cells were lysed in radioimmunoprecipitation assay buffer. Cell lysates were collected by pelleting cell debris, and the concentration of protein was quantified by using a dye-binding assay (Bio-Rad, Hercules, CA). Eighty micrograms of cell lysate was electrophoresed in a sodium dodecyl sulfate/12.5% polyacrylamide gel and electrotransferred to a nitrocellulose membrane. After blocking with phosphate-buffered saline with 0.3% Tween-20 containing 5% skim milk for 1 hour, the membranes were reacted with appropriate antibodies. After washing with phosphate-buffered saline with 0.3% Tween-20, membranes were reacted with horseradish peroxidase–conjugated anti-mouse immunoglobulin G or anti-rab-

bit immunoglobulin G antibodies diluted 1:3000. Membranes were washed again and then visualized with an enhanced chemiluminescence kit (Amersham Pharmacia Biotech, Uppsala, Sweden).

Real-Time Detection Polymerase Chain Reaction

The PCR reaction mixture was prepared by using TaqMan Universal Master Mix (PE Applied Biosystems, Foster City, CA). The primer set applied to amplify La protein messenger RNA (mRNA) consisted of 5′-CGCTGGGAGGTGGAGTCGTT-3′ (exon 1) and 5′-CCCGTGGCAAATTGAAGTCG-3′ (exon 2). The probe, 5′-TGCCCTGGAGGCCAAAATCTGTCATC-3′ (exon 2), was designed to target an internal region between the forward and reverse primers. The primer set for PTB mRNA was 5′-AGCACGCCAAGCTGTCGCT-3′ (exon 8) and 5′-GGAACGGAAAGGCCGAAGG-3′ (exons 8–10). The probe was 5′-ACACACGCCCAGACCTGCCTTCCG-3′ (exon 8). The primer set for eIF3 p170 protein mRNA was 5′-CCGGAAAATGCCCTCAAACTA-3′ (exon 1) and 5′-AAGTGGCTCTTGCGAAGATCCACGC-3′ (exon 7). The probe sequence was 5′-CCAACGAATTTCTTGAGGTT-3′ (exon 2). The primer set for the internal control glyceraldehyde-3-phosphate dehydrogenase mRNA was designed according to GenBank M33197 by using the following primers: exon 7, 5′-TGCACCACCAACTGCTTAGCACCC-3′; and exon 8, 5′-CTTGATGTCATCATATTTGGCAGG-3′. The probe for glyceraldehyde-3-phosphate dehydrogenase-P, designed on the basis of exons 7 and 8, was 5′-TGACCACAGTCCATGCCATCACTGC-3′. Fifty PCR amplification cycles of 95°C for 30 seconds, 60°C for 40 seconds, and 72°C for 30 seconds were repeated by using a real-time PCR system (ABI PRISM 7700 Sequence Detection System; PE Applied Biosystems). To prepare standard RNA, PCR products were cloned into pBluescript vector and linearized at the T3 promoter site. Standard RNA was synthesized by using T7 RNA polymerase and purified by using Isogen (Wako Junyaku, Osaka, Japan) and deoxyribonuclease I (TaKaRa, Shiga, Japan). We detected HCV RNA in liver by using RTD-PCR as previously described.[38]

Statistical Analysis

All data are expressed as means ± SEM. Significance was tested by the Student *t* test and 1-way analysis of variance with Bonferroni's methods.

Results

Gene-Expression Profiling in Confluent or Serum-Starved Cells and the Activities of Hepatitis C Virus Internal Ribosomal Entry Site–Directed Translation

RCF-26 cell lines constitutively express dicistronic RNA transcripts containing sequences encoding the reporter proteins RL and FL separated by a functional HCV IRES (Figure 1). The activities of these proteins expressed in RCF-26 cells reflect cap-dependent and HCV IRES–directed translation, respectively. To rule out the possibility that FL activity from the second cistron reflected the nonspecific ribosomal scanning rather than HCV IRES–directed translation, we evaluated RL and FL activities in ΔRCF-9 cells in which the functional HCV IRES element had been deleted. The ratio of FL to RL (relative HCV IRES activity) in ΔRCF-9 was 2.5% of that in RCF-26, thus reflecting the specificity of HCV IRES activity in RCF-26 cells (Figure 2*B–D*).

To examine the relationship of the cellular proteins that vary in abundance and HCV IRES activities, RCF-26 cells and ΔRCF-9 cells were cultured in 15-cm dishes at confluence or under serum depletion for 48 hours, and changes in cellular gene expression and HCV IRES activities were evaluated. Under these conditions, the cellular DNA content increased at G_0/G_1 phase (49% to 74% in confluent cells and to 59% in serum-starved cells) and decreased at S phase (38% to 18% in confluent cells and to 35% in serum-starved cells) or G_2/M phase (14% to 8% in confluent cells and to 6% in serum-starved cells; Figure 2*A*). The degree of changes during the cell cycle was much greater in the confluent cells than in the serum-starved cells. The activities of HCV IRES–directed translation were reduced to 24% in confluent cells and to 22% in serum-starved cells compared with controls (Figure 2*C* and *D*), whereas the activities of cap-dependent cellular translation were essentially maintained (Figure 2*B*). Neither a significant difference in FL activity nor relative HCV IRES activity was found in ΔRCF-9 under these conditions (Figure 2*C* and *D*).

These results were not due to variations in the RNA stability of the RL and FL reporter genes. Northern blotting of mRNA transcribed from dicistronic constructs containing sequences encoding these 2 reporter proteins did not show either RNA degradation or splicing (data not shown). The relative expression ratio of mRNA of RL to FL determined by cDNA microarray did not change in either confluent or serum-starved cells (Figure 2*E*).

Gene-expression profiling changed in response to these conditions listed in Table 1. Serum proteins such as α_2-macroglobulin and albumin, as well as cell adhesion molecules such as cadherin, major histocompatibility complex, and fibronectin, were up-regulated by more than 1.8-fold. Albumin, a major serum protein that is specifically produced in the liver, was remarkably regulated in a cell-cycle dependent manner. However, cell-cycle and growth-related genes such as cyclin A, cyclin B, CDK1, cell division cell cycle 18, p53, hepatoma-

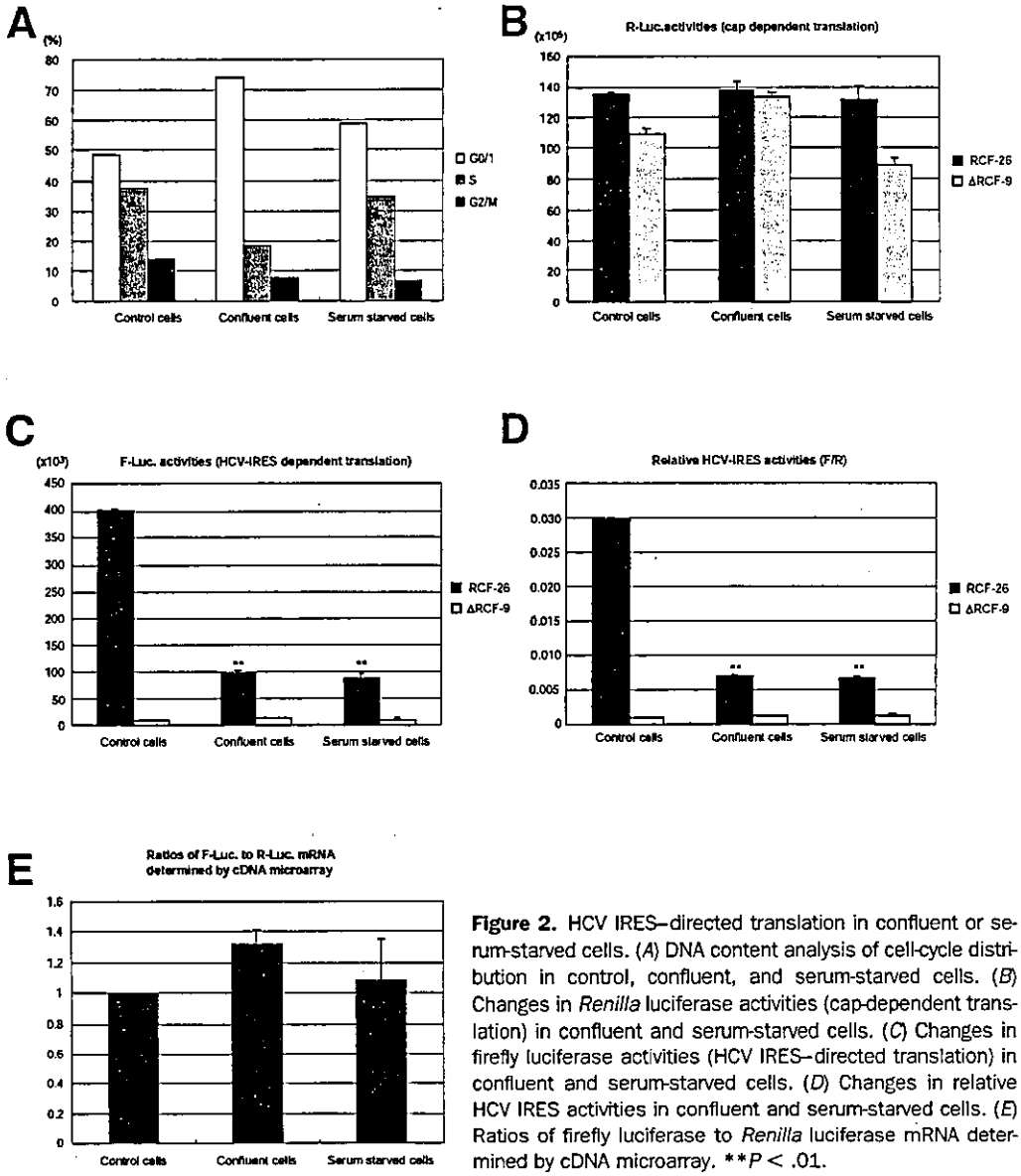

Figure 2. HCV IRES–directed translation in confluent or serum-starved cells. (*A*) DNA content analysis of cell-cycle distribution in control, confluent, and serum-starved cells. (*B*) Changes in *Renilla* luciferase activities (cap-dependent translation) in confluent and serum-starved cells. (*C*) Changes in firefly luciferase activities (HCV IRES–directed translation) in confluent and serum-starved cells. (*D*) Changes in relative HCV IRES activities in confluent and serum-starved cells. (*E*) Ratios of firefly luciferase to *Renilla* luciferase mRNA determined by cDNA microarray. $^{**}P < .01$.

derived growth factor, and nm23 were down-regulated, as were genes related to RNA polymerase, such as RNA polymerase II, subunit 5-mediating protein (RMP), La protein, and topoisomerase II. The La protein binds the stem loop IV structure in HCV IRES and stimulates HCV IRES–directed translation.[16,17] With regard to changes in the expression of canonical and noncanonical initiation factors (Table 2), La protein and PTB expression were repressed in both confluent and serum-starved cells. The expression of eIF3 (p170 and p116) was predominantly repressed in confluent cells, and the expression of eIF2γ was predominantly repressed in serum-starved cells. Conversely, the expression of ribosomal protein S9 and PABPC-1 was induced in confluent cells. The degree to which gene expression changed was more predominant in confluent cells than in serum-starved cells. This might reflect the greater degree of changes in the cell-cycle distribution of G_0/G_1 and S phases in confluent cells than in serum-starved cells (Figure 2*A*). The results of northern blots of La protein, PTB, and albumin expression coincided with these results (Figure 3). We evaluated changes in La protein and PTB expression by using RTD-PCR. The relative expression of La protein in confluent and serum-starved cells was 16% and 33% of control cells, respectively. The relative expression of PTB in confluent and serum-starved cells was 10% and 26% of control cells, respectively (data not shown). These data suggest that several canonical and noncanonical initiation factors, such as La protein, PTB, eIF3, and eIF2γ, are initiation factors responsible for regulating HCV IRES activity in a cell cycle–dependent manner.

Table 1. Up- and Down-regulated Genes in Confluent and Serum-Starved Cells

UniGene	Gene name	Category	Confluent cells	Serum-starved cells	Mean (fold)
Up-regulated					>1.8
Hs.74561	Alpha-2-macroglobulin	Serum protein	12.87 ± 2.13	5.13 ± 0.10	9.00 ± 2.40
Hs.75442	Albumin	Serum protein	6.07 ± 1.07	3.26 ± 0.37	4.67 ± 0.93
Hs.77054	B-cell translocation gene 1	Antiproliferative gene	4.73 ± 1.76	2.97 ± 0.83	3.85 ± 0.94
Hs.82004	Cadherin 1, E-cadherin (epithelial)	Cell adhesion	5.14 ± 2.46	2.36 ± 0.30	3.75 ± 1.29
Hs.2257	Vitronectin	Cell adhesion	3.97 ± 0.68	2.11 ± 0.22	3.04 ± 0.61
Hs.277477	MHC class IC	Cell adhesion	3.26 ± 0.82	2.17 ± 0.09	2.71 ± 0.46
Hs.77961	MHC class IB	Cell adhesion	3.33 ± 0.23	2.08 ± 0.24	2.71 ± 0.39
Hs.1119	TR3 orphan receptor	Receptor	3.38 ± 1.23	1.95 ± 0.23	2.66 ± 0.66
Hs.1665	Zinc finger transcriptional regulator	Transcription factor	2.66 ± 0.40	2.53 ± 0.40	2.60 ± 0.23
Hs.287820	Fibronectin gene	Cell adhesion	2.40 ± 0.77	2.11 ± 0.34	2.26 ± 0.36
Hs.2780	JunD	Oncogene	2.23 ± 0.39	1.99 ± 0.54	2.11 ± 0.28
Down-regulated					<0.55
Hs.89525	Hepatoma-derived growth factor	Cell growth	0.67 ± 0.27	0.42 ± 0.08	0.55 ± 0.13
Hs.7943	RMP	RNA polymerase II binding	0.44 ± 0.09	0.64 ± 0.07	0.54 ± 0.07
Hs.23960	Cyclin B	Cell cycle	0.44 ± 0.25	0.62 ± 0.17	0.53 ± 0.13
Hs.118638	Nm23A	Cell growth	0.52 ± 0.01	0.53 ± 0.11	0.52 ± 0.05
Hs.83715	Autoantigen La	RNA polymerase III synthesis	0.43 ± 0.06	0.61 ± 0.01	0.52 ± 0.06
Hs.16297	COX17	Cytochrome-c-oxidase	0.47 ± 0.14	0.55 ± 0.06	0.51 ± 0.07
Hs.95577	CDK1	Cell cycle	0.36 ± 0.02	0.65 ± 0.07	0.50 ± 0.09
Hs.174017	Topoisomerase (DNA) II alpha	RNA polymerase II holoenzyme	0.44 ± 0.11	0.55 ± 0.08	0.50 ± 0.05
Hs.85137	Cyclin A	Cell cycle	0.42 ± 0.03	0.56 ± 0.17	0.49 ± 0.08
Hs.9235	Nucleoside-diphosphate kinase	Cell growth	0.51 ± 0.08	0.46 ± 0.05	0.49 ± 0.04
Hs.75133	Transcription factor 6–like 1	Transcription factor	0.40 ± 0.07	0.57 ± 0.18	0.48 ± 0.09
Hs.69563	Cell division cycle 18	Cell cycle	0.45 ± 0.04	0.51 ± 0.09	0.48 ± 0.04
Hs.58593	RAP30	Transcription factor	0.37 ± 0.02	0.58 ± 0.00	0.48 ± 0.06
Hs.75323	Prohibitin	Antiproliferative gene	0.50 ± 0.01	0.39 ± 0.01	0.44 ± 0.03
Hs.1846	p53	Cell cycle	0.66 ± 0.18	0.22 ± 0.04	0.44 ± 0.15
Hs.111758	Keratin 6	Housekeeping	0.24 ± 0.02	0.63 ± 0.07	0.43 ± 0.12
Hs.78271	Keratin 8	Housekeeping	0.33 ± 0.18	0.53 ± 0.08	0.43 ± 0.10
Hs.748	Fibroblast growth factor receptor 1	Cell growth	0.39 ± 0.12	0.30 ± 0.05	0.34 ± 0.06

Hepatitis C Virus Internal Ribosome Entry Site Activity at Different Phases of the Cell Cycle

We examined the relationship between HCV IRES activity and cell division in more detail. We synchronized cell-cycle progression and compared the production of RL and FL reporter proteins during different phases of the cell cycle. Cells were blocked at the G_1/S interface by adding aphidicolin to the culture medium and were then released from the aphidicolin

Table 2. Up- and Down-regulated Initiation Factors in Confluent and Serum-Starved Cells

UniGene	Gene name	Confluent cells	Serum-starved cells	Mean (fold)
Hs.180920	Ribosomal protein S9	1.92 ± 0.01	1.11 ± 0.18	1.51 ± 0.24
Hs.172550	Polypyrimidine tract binding protein (PTB)	0.62 ± 0.17	0.62 ± 0.03	0.62 ± 0.07
Hs.83715	La protein	0.43 ± 0.06	0.61 ± 0.01	0.52 ± 0.06
Hs.2730	Heterogeneous nuclear ribonucleoprotein L (RNPL)	1.23 ± 0.33	1.02 ± 0.13	1.13 ± 0.16
Hs.63525	Poly(rC)-binding protein 2 (PCBP2)	1.20 ± 0.11	0.95 ± 0.10	1.07 ± 0.09
Hs.172182	Poly(A)-binding protein, cytoplasmic 1	1.87 ± 0.62	1.19 ± 0.05	1.53 ± 0.32
Hs.183418	Cell division cycle 2–like 1 (PITSLRE proteins)	0.85 ± 0.10	0.70 ± 0.07	0.78 ± 0.07
Hs.198899	eIF3-p170	0.47 ± 0.28	1.10 ± 0.36	0.79 ± 0.26
Hs.57783	eIF3-p116	0.58 ± 0.12	0.70 ± 0.02	0.64 ± 0.06
Hs.4310	eIF1A	0.84 ± 0.06	0.89 ± 0.17	0.86 ± 0.07
Hs.151777	eIF2A	1.37 ± 0.20	1.59 ± 0.20	1.48 ± 0.13
Hs.12163	eIF2β	0.88 ± 0.10	0.94 ± 0.02	0.91 ± 0.04
Hs.211539	eIF2γ	1.31 ± 0.03	0.61 ± 0.17	0.96 ± 0.22
Hs.129673	eIF4A	1.05 ± 0.09	0.81 ± 0.07	0.93 ± 0.08
Hs.93379	eIF4B	1.38 ± 0.48	0.94 ± 0.20	1.16 ± 0.25
Hs.79306	eIF4E	0.86 ± 0.14	0.83 ± 0.01	0.84 ± 0.06
Hs.286236	eIF5	0.91 ± 0.02	1.23 ± 0.35	1.07 ± 0.17

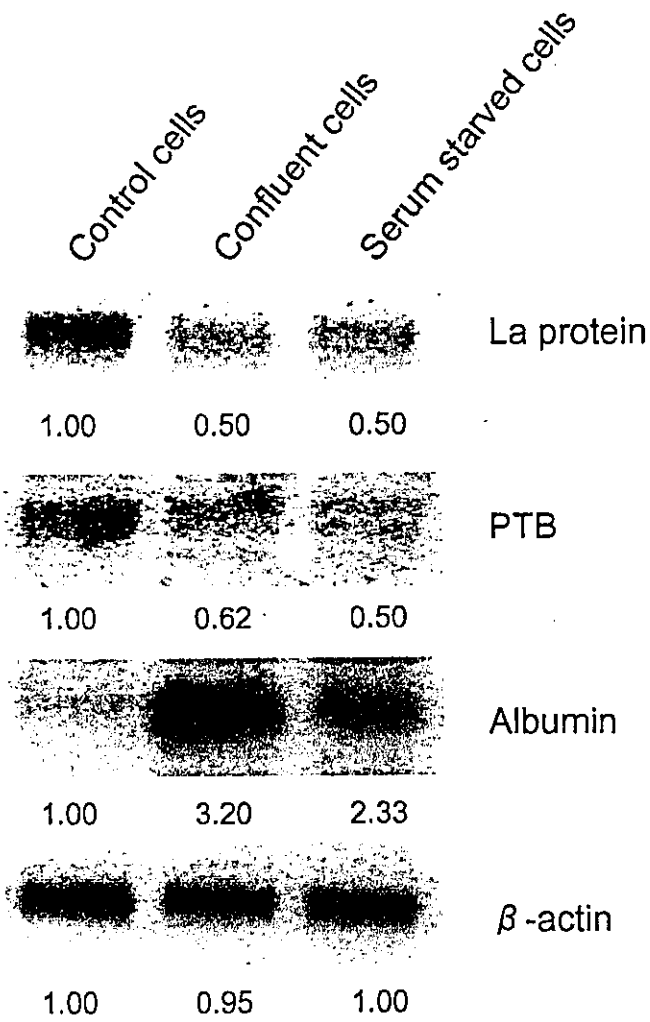

Figure 3. Northern blotting of La protein, PTB, and albumin in RCF-26. Expression of La protein and PTB is repressed in confluent and serum-starved cells, whereas albumin expression is significantly up-regulated.

block. Synchronized cells subsequently moved into the S and G_2/M phases of the cell cycle and then returned to G_1/S phase at approximately 27 hours, as determined by the cellular DNA content measured by flow cytometry (Figure 4*A*). RL activities increased proportionally, reflecting the increased number of cells after division. The cell number doubled at approximately 27 hours after 1 round of the cycle was completed. Conversely, HCV IRES activity varied with cell cycle, and the ratio of FL to RL (relative HCV IRES activity) increased during and immediately after G_2/M phase (12–18 hours after release from aphidicolin). The relative HCV IRES activity decreased by 36 hours after release (Figure 4*C*), corresponding to reentry into the G_0 and G_1 phases. However, the HCV IRES activity increased again, starting at approximately 39 hours, probably because many cells continued into a second cycle (Figure 4*A* and *C*). No significant differences in relative HCV IRES activity were found in ΔRCF-9 cells up to 30 hours after release (Figure 4*C*).

Gene-Expression Profiles in Cells Undergoing Cell-Cycle Progression

To determine which host factors are involved in this cell cycle–dependent regulation of HCV IRES activity, we evaluated gene-expression profiles in cells undergoing cell-cycle progression. Total RNA was extracted from synchronized cells at 3, 9, 15, 18, 24, 30,

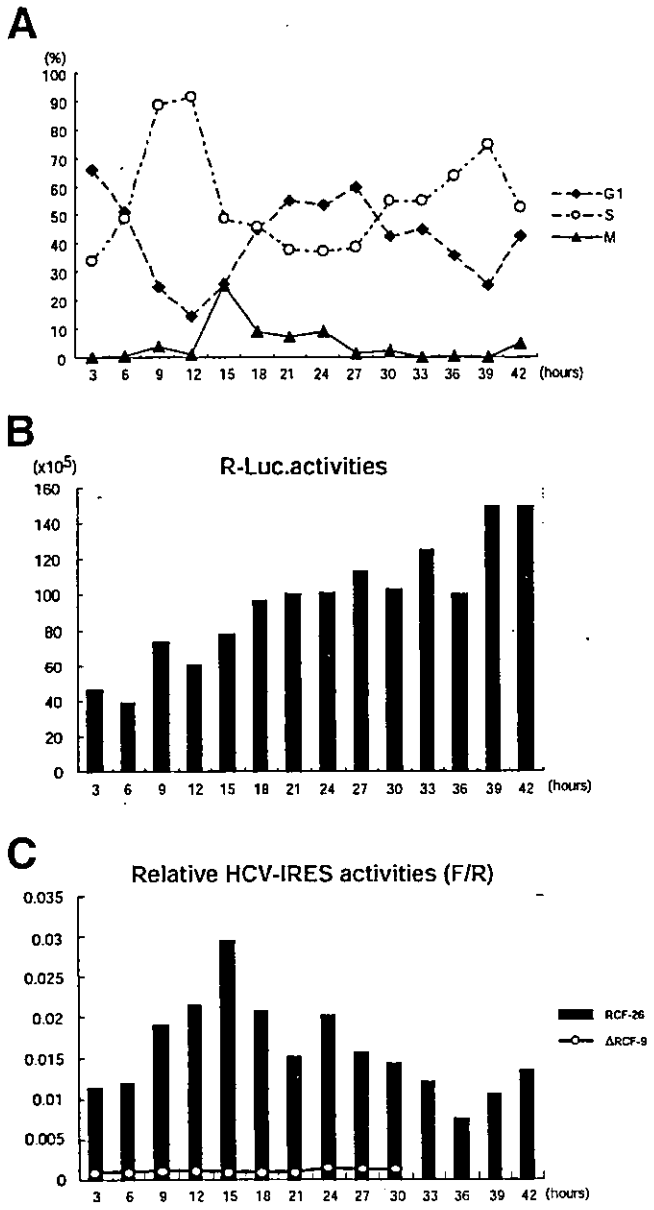

Figure 4. HCV IRES activity and cell-cycle progression. (*A*) Changes in distribution with cell-cycle progression. Proportions of G_1, S, and G_2/M are individually shown. (*B*) Changes of *Renilla* luciferase activities (cap-dependent translation) with cell-cycle progression. (*C*) Changes in relative HCV IRES activities (firefly to *Renilla* luciferase activities; FL/RL) with cell-cycle progression. HCV IRES activity varied with cell cycle in RCF-26 cells but did not change in ΔRCF-9 cells.

36, and 42 hours after release from the aphidicolin block (G_1/S border) and was analyzed with the cDNA microarray. We constructed a 1-dimensional SOM to evaluate changes in gene expression (Cluster and Tree view; http://www.microarrays.org/software/html) (Figure 5). We identified 3 large gene clusters as the cell cycle progressed. The first cluster of genes was induced at S phase (at 3 to 9 hours). The second and third clusters were induced at G_2/M (at 15–18 hours) and at G_1 (at 24 to 36 hours), respectively. Most of the HCV IRES–related canonical and noncanonical initiation factors were induced during S and G_2/M phases. PCBP-2, PTB, eIF3 (p110 and p170), eIF2γ, and eIF2β were induced during S phase, whereas La protein and RNPL were induced during G_2/M. These factors bind HCV IRES structure or have functional relevance to HCV IRES activity. Conversely, PABPC-1, eIF4A, and eIF4B were induced during G_1 phase. These factors are not required for HCV IRES–directed translation but are necessary for cap-dependent translation.[39] The induction of the ribosomal protein S9 in G_1 phase was a controversial finding because S9 was reported to bind stem loop IIId of HCV IRES. The functional role of the ribosomal protein S9 is discussed later. In cells, translation takes place immediately in the presence of mRNA, and luciferase activity could be detected within 30 seconds from the initiation of the translation. Thus, the induction of canonical and noncanonical initiation factors related to HCV IRES during S and G_2/M phases contributed to cell cycle–dependent regulation of translation directed by HCV IRES (Figure 5).

We evaluated changes in La protein expression determined by the cDNA microarray by using RTD-PCR (Figure 6). The changes in HCV IRES–directed translation and in La protein expression closely correlated (Figure 6).

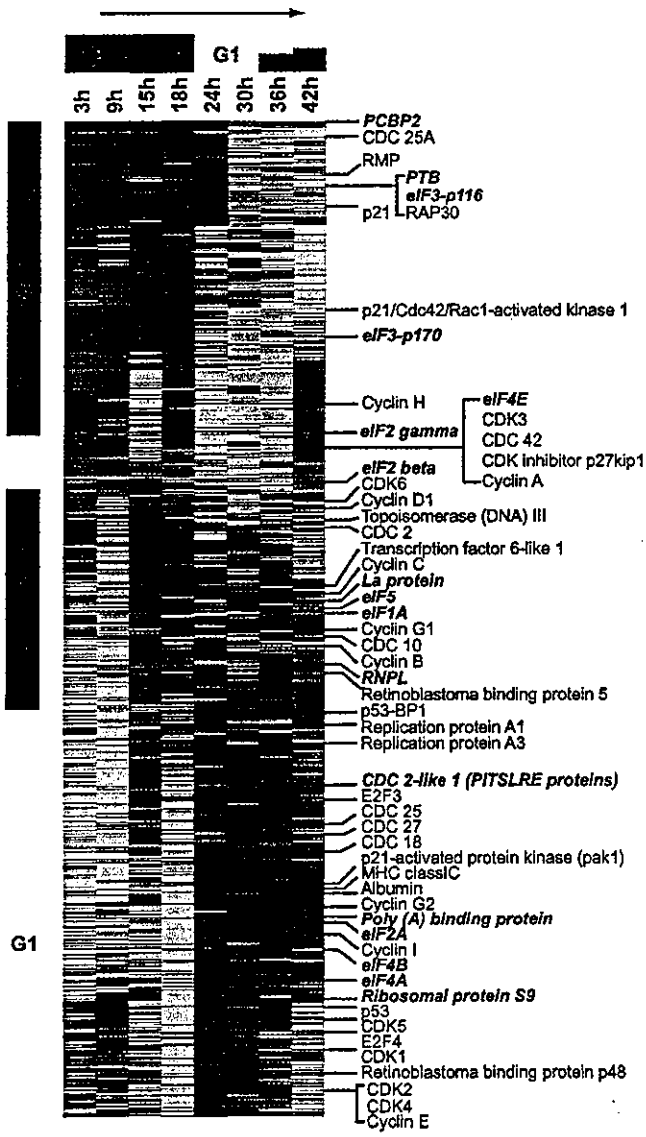

Figure 5. Gene-expression profiling in RCF-26 cells undergoing cell-cycle progression. RCF-26 cells were synchronized at the G_1/S border with aphidicolin. After release from aphidicolin block, the cell cycle progressed to S phase at 3–6 hours and G_2/M phase at 15–18 hours and returned to G_1 phase at 24–30 hours. Cells were harvested at 3, 9, 15, 18, 24, 30, 36, and 42 hours and analyzed with cDNA microarray, and then an SOM was constructed by using Cluster (Stanford University). Gene clusters up-regulated in the S, G_2/M, and G_1 phases (*red*) were detected with cell-cycle progression. Canonical and noncanonical initiation factors and cell cycle–related genes are listed (*right*).

Functional Analysis of the Effect of HCV IRES–Related Canonical and Noncanonical Initiation Factors on Translation Directed by HCV IRES

To prove that the induction of the canonical and noncanonical initiation factors during S and G_2/M phases contributes to cell cycle–dependent translation of HCV, antisense phosphorothioate oligos were designed for La protein, PTB, eIF3 p170, eIF2γ, RNPL, PABPC-1, PCBP-2, and ribosomal protein S9, and HCV IRES activity was evaluated under the suppression of these factors. RT-PCR showed that expression of the targeted factors was significantly reduced by the antisense oligos, whereas that of β-actin did not significantly change (Figure 7*B*). Reduced expression of these factors was also evaluated by Western blotting (Figure 7*C*). The suppression of La protein, PTB, and eIF2γ specifically reduced HCV IRES activity to 40%, 50%, and 53% of the control level, respectively. The effect of inhibiting HCV IRES activity was equal to or greater than that exerted by an antisense oligo against 5′-NTR of HCV (nt 330–350). However, suppression of eIF3 p170, RNPL, PABPC-1, PCBP-2, and ribosomal protein S9 did not reduce HCV IRES activity (Figure 7*A*). To rule out the

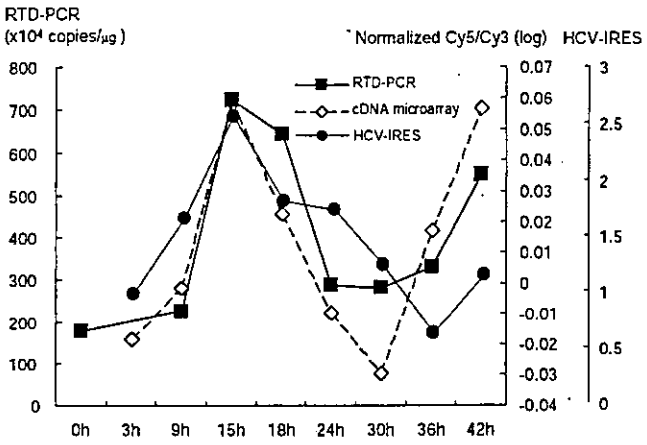

Figure 6. La protein expression in RCF-26 under cell-cycle progression determined by RTD-PCR. Normalized Cy5/Cy3 of mRNA expression of La protein and HCV IRES activities are shown in same dimension.

possibility that these reduced HCV IRES activities were not due to nonspecific suppression by the antisense oligos, antisense oligos to La protein, PTB, eIF3 p170, and ribosomal protein S9 were applied to ΔRCF-9 in which the functional HCV IRES element had been deleted. Two antisense oligos to La protein and PTB, which reduced HCV IRES activity in RCF-26, did not change HCV IRES activity in ΔRCF-9. Similarly, 2 antisense oligos to eIF3 p170 and ribosomal protein S9, which had no effect on HCV IRES activity, did not have any effect on HCV IRES activity in ΔRCF-9 (Figure 7*A*). Conversely, overexpression of La protein, PTB, and eIF3 p170 significantly enhanced HCV IRES activity in a dose-dependent manner, whereas the overexpression of eIF2γ, RNPL, PCBP-1, PCBP-2, and ribosomal protein S9 had no effect (Figure 8). The overexpression of La protein, PTB, and eIF3 p170 in ΔRCF-9 did not have any effect on HCV IRES activity (Figure 8). We also confirmed these findings in rabbit reticulocyte lysates by co-translating pRL-HL (HCV IRES reporter) and La protein, PTB, and eIF3 p170 (data not shown). Thus, of these HCV IRES–related canonical and noncanonical initiation factors, La protein and PTB significantly changed HCV IRES activity in both the suppressed and overexpressed states. Thus, changes in the expression of these factors alter HCV IRES activity in a cell cycle–dependent manner.

Expression of La Protein, Polypyrimidine Tract Binding Protein, and Eukaryotic Initiation Factor 3 in Lesions of Chronic Hepatitis C

To examine the functional role of these factors on HCV replication in the lesions of chronic hepatitis C, we evaluated their expression in 26 liver samples from patients with chronic hepatitis C and in 8 normal liver samples by RTD-PCR. Tables 3 and 4 list the clinical characteristics of the patients. The expression level of La protein in the specimens of the patients with chronic hepatitis C was significantly higher than that of the normal livers, whereas the expression of PTB and eIF3 p170 was not statistically different (Table 3). Some of these samples were also reevaluated by Northern blotting, and the results were similar (data not shown). Up-regulation of the La protein was related to neither the histological stage nor the activity of liver disease (Table 4). However, the expression of La protein was significantly correlated with the amount of HCV RNA in the liver (Figure 9). Moreover, HCV RNA replication was significantly higher in liver with high La protein expres-

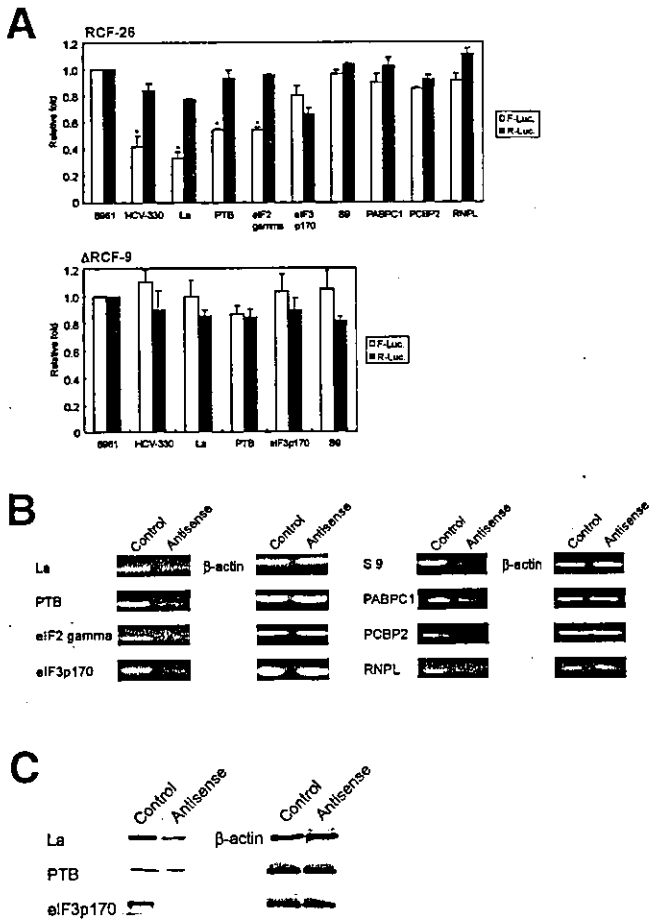

Figure 7. Suppression of HCV IRES–related canonical and noncanonical initiation factors (La protein, PTB, eIF3 [p170], eIF2γ, RNPL, PABPC-1, PCBP-2, and ribosomal protein S9) by specific antisense phosphorothioate oligos and HCV IRES activity in RCF-26 and ΔRCF-9. (*A*) Changes in *Renilla* (cap-dependent translation) and firefly luciferase (HCV IRES–directed translation) activities caused by suppression of these factors by antisense phosphorothioate oligos. $*P < .05$. (*B*) Suppression of factors confirmed by RT-PCR. (*C*) Suppression of factors confirmed by Western blotting.

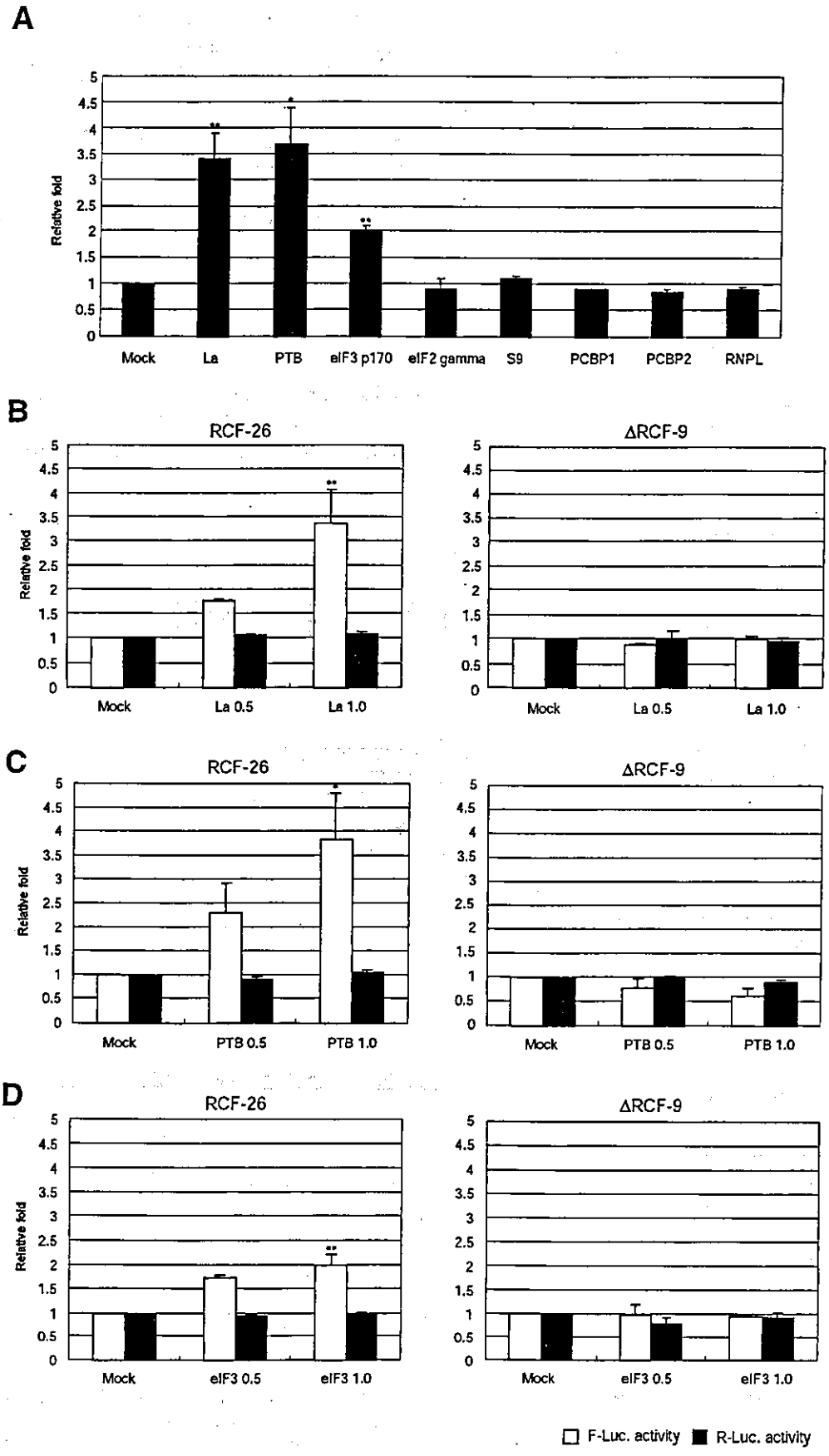

Figure 8. (*A*) Overexpression of HCV IRES–related canonical and noncanonical initiation factors (La protein, PTB, eIF3 [p170], eIF2γ, RNPL, PCBP-1, PCBP-2, and ribosomal protein S9) in RCF-26 and HCV IRES activity. (*B–D*) Dose-dependent overexpression of La protein, PTB, and eIF3 p170 in RCF-26 and ΔRCF-9. $*P < .05$; $**P < .01$.

Table 3. Expression of La Protein, PTB, and eIF3 (p170) in Liver Detected by RTD-PCR

Diagnosis	n	Age (y)	Sex (M:F)	ALT (*IU/L*)	Serological HCV type (group 1:group 2)	La (×10^6 *copies/μg*)	PTB-1 (×10^5 *copies/μg*)	eIF3 (p170) (×10^6 *copies/μg*)
Normal	8	64.5 ± 4.10	5:3	17.0 ± 9.86	ND	1.08 ± 0.11	1.34 ± 0.15	3.32 ± 0.46
Chronic hepatitis C	26	62.8 ± 2.27	20:6	67.7 ± 10.2[a]	21:3[b]	2.75 ± 0.26[c]	1.40 ± 0.14	2.21 ± 0.31

ALT, alanine aminotransferase; ND, not done.
[a]$P < .05$.
[b]Two patients were unclassified.
[c]$P < .01$.

sion (Figure 10). These findings indicate that La protein plays an important role in the replication of HCV in the livers of patients infected with chronic hepatitis C.

Discussion

Although extensive studies have examined the molecular biology of HCV, the responsible host factors that regulate HCV replication in patients with chronic hepatitis C have not yet been elucidated. Patients with a high viral load are refractory to interferon therapy, even when it is combined with ribavirin.[3–6] Recent advances in the HCV replicon system have shown some adaptive mutations in the HCV genome (NS5A or NS3) for efficient replication of cellular factors that inhibit HCV replication, such as PKR and interferon-regulatory protein 1.[40] However, there has been no clear evidence that these factors are truly determinant of HCV replication in patients with chronic hepatitis C. The identification of host factors that regulate HCV replication in vivo should show the underlying mechanism of high viral load in patients with chronic hepatitis C. Moreover, it could provide a basis for the development of a new antiviral treatment strategy.

The translation of viral polyprotein is an important step in viral replication and could thus present a target for a novel antiviral therapy. Translation of the HCV RNA genome is initiated by a highly structured RNA segment, the IRES, that occupies most of the 5′-NTR RNA.[7–15] We showed that HCV IRES activity varies during different phases of the cell cycle: it is highest during the S and M phases and lowest during the G_0 phase of the cell cycle.[22] These findings have important clinical relevance because viral translation might be enhanced by factors that stimulate the regeneration of hepatocytes in patients with chronic hepatitis C. We investigated the molecular basis of these findings and found host factors that regulate HCV IRES.

The expression of La protein, PTB, eIF3, and eIF2γ was repressed in confluent and serum-starved cells, but eIF3 and eIF2γ were reduced in confluent or serum-starved cells. Analysis of cell-cycle progression more precisely showed the interaction of these initiation factors with the cell cycle–dependent regulation of HCV IRES activity. Most of the HCV IRES–related canonical and noncanonical initiation factors (PCBP-2, PTB, eIF3, eIF2γ, eIF2β, La protein, and RNLPL) were induced during the S and G_2/M phases of the cell cycle. Conversely, eIF4A, eIF4B, and PABPC-1, which are not supposed to be a requirement for HCV IRES activity,[33,39] were induced during G_1. In cells, because protein translation takes place immediately in the presence of mRNA, dynamism of expression profiles might directly link to HCV IRES activity, although some protein levels were also regulated by the posttranslational modification. The finding that HCV uses host factors induced during cell division (S and G_2/M), but not during quiescence (G_0/G_1), is of interest. In this respect, HCV IRES–directed translation differed from either cap-dependent or IRES-directed translation by encephalomyocarditis virus and the picornavirus-like group. Reports indicate that eIF4B and PABPC-1 are required for encephalomyocarditis virus and poliovirus, but not for HCV translation.[39] G_1 induction of the ribosomal protein S9, which supposedly binds the secondary structure of HCV IRES,[7] seems controversial. To further investigate these findings, we evaluated the functional roles of these factors in HCV IRES activity. Among the canonical and noncanonical HCV IRES–related initiation factors, the suppression of PTB, La protein, and eIF2γ by using antisense oligos reduced HCV IRES activity, and the overexpression of PTB, La, and eIF3 stimulated HCV IRES activity. The La protein and PTB changed HCV IRES activity in both

Table 4. Histological Findings and La Protein Expression

Histology	n	La (×10^6 *copies/μg*)
F1	2	1.98 ± 0.03
F2	6	3.31 ± 0.80
F3	7	3.04 ± 0.48
F4	11	2.40 ± 0.30
A1	10	2.72 ± 0.52
A2	15	2.82 ± 0.30
A3	1	1.86